

**Solar Energy Conversion and Storage by Photoswitchable Organic Materials in Solution, Liquid, Solid, and Changing Phases**

Journal:	<i>Journal of Materials Chemistry C</i>
Manuscript ID	TC-REV-03-2021-001472.R1
Article Type:	Review Article
Date Submitted by the Author:	27-Apr-2021
Complete List of Authors:	Qiu, Qianfeng; Brandeis University Department of Chemistry, Chemistry Shi, Yuran; Brandeis University Department of Chemistry, Chemistry Han, Grace; Brandeis University, Chemistry

1 Solar Energy Conversion and Storage by Photoswitchable 2 Organic Materials in Solution, Liquid, Solid, and 3 Changing Phases

4 Qianfeng Qiu, Yuran Shi, and Grace G. D. Han*

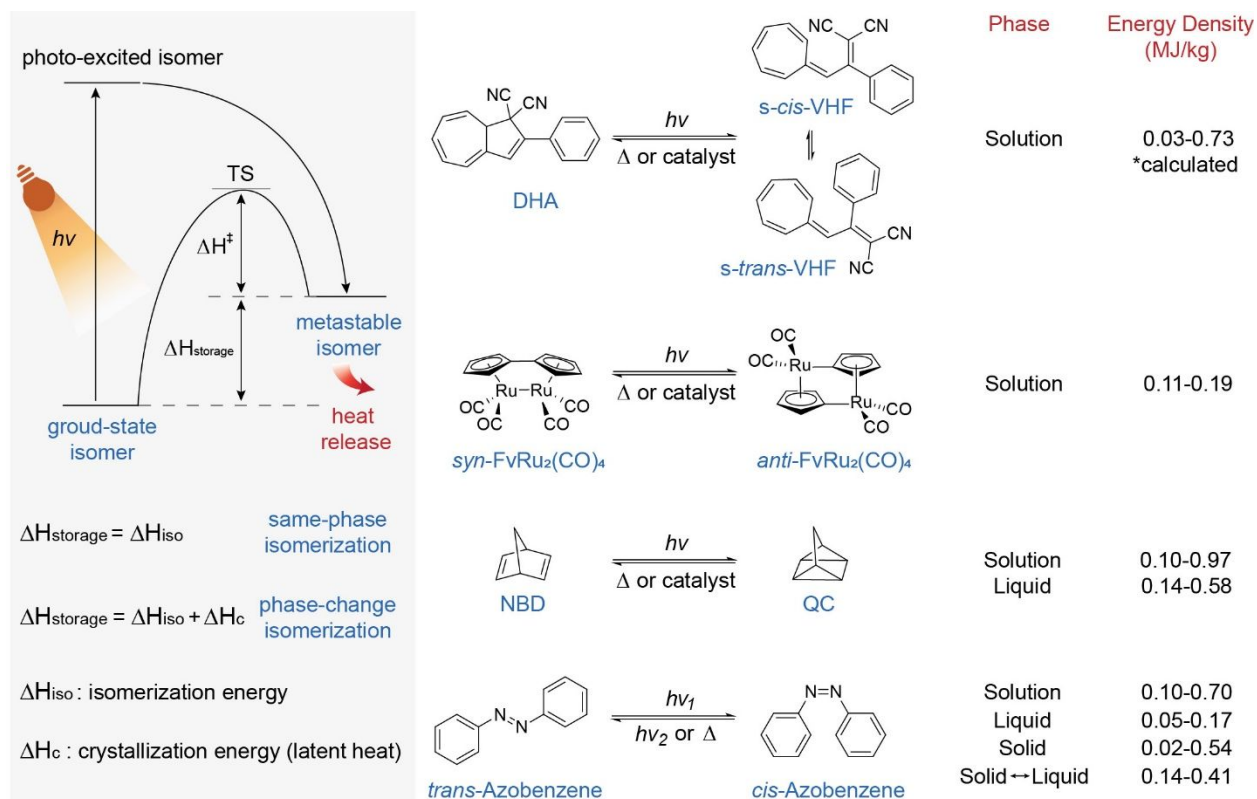
5 Department of Chemistry, Brandeis University, 415 South Street, Waltham, MA 02453, USA

6 Email: gracehan@brandeis.edu

8 **Abstract**

9
10 This review illustrates various structural design principles for molecular solar thermal (MOST)
11 energy storage materials based on photoswitches that operate in different conditions, *e.g.* solution
12 state, neat liquid, and solid, or result in a solid-liquid phase transition during their photo-
13 isomerization. The structural modifications of MOST compounds enable the formation of each
14 phase, which also influences the important performance metrics of the photoactive energy
15 materials: the energy storage density per molecule or gravimetric energy density. Other major
16 optical and thermal properties are also modulated by the molecular designs and affect the energy
17 storage period, efficiency of the system, and device structures that accommodate the solar energy
18 storage in each form of the MOST compounds. The introduction of different strategies that enable
19 the large density heat storage in specific phase conditions will help to facilitate the further
20 development of efficient MOST systems that will be readily integrated to device-scale applications
21 with a transformative impact on the renewable energy markets.

22

1 **1. Introduction**

2
3 **Figure 1.** Photon energy storage process, classes of MOST compounds, their isomerization
4 reactions, and the range of their energy densities reported in the corresponding phases.

5
6 Molecular solar thermal (MOST) materials, composed of photo-switching molecules that respond
7 to light and isomerize into a metastable conformer, have been investigated as a promising
8 candidate that stores photon energy in chemical bonds and releases the energy in the form of heat
9 upon triggering. Among many of novel photoswitching compounds developed to undergo either
10 *trans-cis* or ring opening-closing isomerization, four of the following compounds have been
11 extensively studied for the energy storage capabilities: 1. dihydroazulene/vinylheptafulvene
12 (DHA/VHF) couples,¹⁻⁵ 2. Fulvalene dimetal complexes, notably $\text{FvRu}_2(\text{CO})_4$,⁶⁻⁸ 3.
13 norbornadiene/quadracyclane (NBD/QC) couples,^{9,10} and 4. azobenzene systems.^{11,12} These

1 molecular systems are reported to store a significant amount of energy in their metastable isomeric
2 forms (on the right side of the equilibrium) obtained by the photo-irradiation of ground-state
3 isomers (on the left side) as shown in Figure 1. The phases in which the photo-activation is
4 performed are described for each category of MOST systems, and the ranges of attainable energy
5 density for each phase are shown. This illustrates the stages of development for each MOST system
6 towards the practical applications which span from solution-state or liquid-based flow systems for
7 solar water heating¹³ and thermal control of building environment^{9,14} to solid-state films for
8 window coatings¹⁵ and polymeric fibers for the integration to smart fabrics.¹⁶ It is crucial to design
9 MOST materials that operate in a certain phase that is required for each application, thus there has
10 been extensive research on the molecular designs that allow the compounds to form a desired phase,
11 switch within the phase, or undergo phase transitions while switching. In this review, we primarily
12 focus on the design strategies of MOST compounds that isomerize in various conditions (*i.e.*
13 solution-state, neat liquid phase, solid phase, and solid-liquid phase transition) and how such
14 molecular designs impact the energy storage in the respective MOST system.

15 We note that the MOST systems based on DHA/VHF report high energy densities up to
16 0.73 MJ/kg according to the computational evaluation of their isomerization energy.¹ DHA
17 undergoes a photo-activated ring opening to form VHF isomers that are under equilibrium between
18 *s-cis* and *s-trans* conformation, and the heat release is triggered by the thermal activation or
19 catalysis of the ring closure of VHF. The unidirectional photo-switching from DHA to VHF and
20 the full back isomerization in dark indicate a remarkable potential of the molecular system for
21 photon energy storage.^{17,18} Various molecular design principles have been explored through the
22 chemical modification of the DHA/VHF scaffold, which improves their optical properties, thermal
23 half-life of VHF, and the energy density of the system. The examples include the substitution of

1 various electron-donating and withdrawing groups on the photoswitch core,^{3,19–23} the conjugation
2 of DHA/VHF scaffold with other photoswitches such as diarylethene and norbornadiene,^{23,24} and
3 controlling aromaticity of the system,^{5,25} protonation-deprotonation process,²⁶ and the strain of
4 macrocycles containing DHA/VHF.²⁷ Although the synthesis of these compounds and their
5 solution-state photoswitching and thermal reversion properties have been elucidated, the
6 experimental measurement of their thermal energy storage densities has remained a challenge,
7 primarily due to the concomitant melting and heat release process occurring at an elevated
8 temperature, which makes it difficult to quantify the exothermicity of the VHF-to-DHA
9 isomerization. This review primarily focuses on the experimental demonstrations of the
10 photoswitching in different phases and the measurement of thermal energy released from MOST
11 systems in such phases. Therefore, the DHA/VHF compounds are not further illustrated here, and
12 we direct the readership to a recent review that discusses the design strategies of DHA/VHF
13 systems for enhancing MOST-relevant properties and calculated energy densities.²⁸ FvRu₂(CO)₄
14 systems undergo the cleavage and reformation of Ru–Ru and C–Ru bonds upon the light
15 irradiation, storing the photon energy in the metastable *anti* conformer which can be thermally
16 reversed or catalyzed to release energy.^{6,29} Various solution-state studies have characterized the
17 optical and thermal properties of FvRu₂(CO)₄ systems.^{7,8,30–34} NBD undergoes a photoinduced
18 [2+2] cycloaddition to convert into its valence isomer QC.^{35–37} The strained QC molecules store a
19 significant amount of energy up to 0.97 MJ/kg which can be released in the form of heat upon
20 thermal activation or catalysis of QC-to-NBD reversion.³⁸ Both highly concentrated solutions and
21 neat liquid phase of materials have been reported to show facile switching and heat release.^{13,39–41}
22 Azobenzene derivatives exhibit reversible photo-isomerization between ground-state *trans* and
23 metastable *cis* forms. Pristine azobenzene and many of its derivatives absorb UV range ($h\nu_1$) to

1 promote *trans*-to-*cis* isomerization, and the reverse isomerization is generally triggered by visible
2 light ($h\nu_2$) for releasing the energy.^{12,42} However, recent studies have successfully demonstrated
3 the separation of the $n-\pi^*$ absorption bands between *trans* and *cis* isomers in the visible light
4 range, enabled by the covalent functionalization of the *ortho* positions of the photochrome, thus
5 achieving a complete cycle of energy storage and release in the absence of UV sources.^{43,44} The
6 energy storage in azobenzene and azoheteroarene systems have been successfully tested in
7 solutions, neat liquid phase, and solid phase. Moreover, the isomerization-induced phase transition
8 between solid (*trans*) and liquid (*cis*) phase has emerged as a novel strategy for enhancing the
9 energy storage in materials, resulting from the phase transition enthalpy contributing to the total
10 energy density in addition to the isomerization energy.¹²

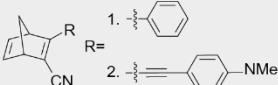
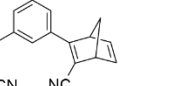
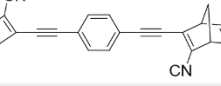
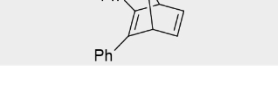
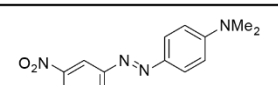
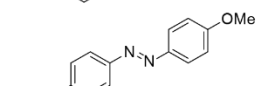
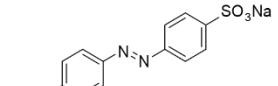
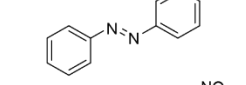
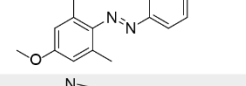
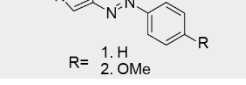
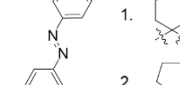
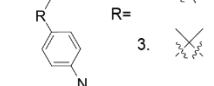
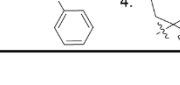
11 In order to develop an ideal MOST system, the research community has pursued diverse
12 approaches of fulfilling the following criteria:^{45,46} high quantum yields of isomerization, high
13 photostationary state (PSS) ratios between ground-state and metastable-state isomers, significant
14 overlap between absorption spectra of photochromes and the solar spectrum, spectral separation
15 between two isomers, high thermal stability of the metastable isomers (*i.e.* a long thermal half-life,
16 $t_{1/2}$), etc. These optical and thermal parameters will be discussed along with the structural designs
17 that enable the conformational change of molecules in each phase, particularly in condensed
18 phases where the intermolecular interaction and steric hindrance play a significant role. Also, the
19 molecular weight of a MOST system is an important factor that determines the gravimetric energy
20 density (MJ/kg) of the system, which is defined as the total energy stored in the unit mass of the
21 materials. Thus, the relative mass ratio between photoactive moieties (energy storage units) and
22 photo-inactive structures (no energy storage; contribution to the total weight) is one of the major

1 metrics that are optimized for MOST compounds. Further discussions on the molecular weight
2 and efficient templating strategy are illustrated in section 4.

3 The molecular designs related to some of these features will be highlighted in the examples
4 that are categorized into four groups according to the phases in which the photon energy storage
5 is performed (solution, condensed liquid, and solid state) as well as the phase that transforms along
6 with photo-switching (between solid and liquid). In addition, the design principles of MOST
7 compounds, which result in a particular phase of materials (liquid, solid, or reversible transition
8 between those), will be described in the respective sections.

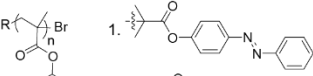
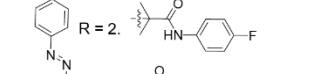
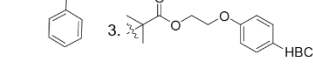
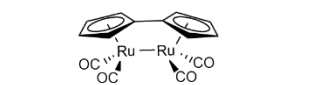
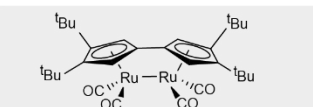
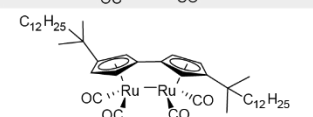
9

1 **2. Solution-state MOST compounds**2 **Table 1. Solution-state properties of MOST materials**

Chemical Structure	MW (g/mol)	Solvent	λ_{\max} (nm)	$\Delta H_{\text{storage}}$ (kJ/mol)	$\Delta H_{\text{storage}}$ (MJ/kg)	$t_{1/2}$ 298 K	Ref.
	92	benzene or isopentane	<250	89	0.97	> 14 h (413 K)	38, 45
	193	DCM	309	122	0.63	55 d	39
	260	DCM	398	103	0.40	5.0 h	
	308	CDCl_3	308	86 ^a	0.56	49 d (QC-QC)	40
	356	CDCl_3	359	92 ^a	0.51	4.3 h (QC-QC)	
	244	toluene	308	86	0.35	43 d	13
	360	toluene	240	85	0.24	6.3 h	
	388	toluene	~242	68	0.18	7.7 h	51
	445	toluene	~245	46	0.10	2.3 d	
	270	toluene	428	98	0.36	0.2 h	
	242	toluene	358	80	0.33	9.6 h	
	327	acetone	420	94	0.29	9.6 h	52
	182	n-heptane	317	49	0.27	4.2 d	
	285	acetone	377	30	0.10	1.9 h	
	186	water	328	38	0.21	3.8 y	57
	216	water	347	38	0.18	47 d	
	444	DCM	~325	55 ^a	0.25	/	
	430	DCM	~325	49 ^a	0.23	/	58
	404	DCM	~325	44 ^a	0.22	2.4 h (323K)	
	458	DCM	~325	45 ^a	0.20	/	

3
4

1 **Table 1.** Solution-state properties of MOST materials (continued)

Chemical Structure	MW (g/mol)	Solvent	λ_{\max} (nm)	$\Delta H_{\text{storage}}$ (kJ/mol)	$\Delta H_{\text{storage}}$ (MJ/kg)	$t_{1/2}$ 298 K	Ref.
	266 ^b	THF	320	186 ^a	0.70	3.1 d	
	266 ^b	THF	/	168 ^a	0.63	/	59
	266 ^b	THF	/	121 ^a	0.46	/	
	442	THF	~400	83	0.19	/	6
	668	THF	~350	88	0.13	/	7
	863	toluene or THF	333	99	0.11	/	8

2
3 a: per unit energy density, b: Repeating unit MW, HBC: hexa-*peri*-hexabenzocoronene, /: unreported

5 Solution-state MOST systems are photoswitching compounds investigated in a respective solvent,
6 as illustrated in Table 1, where the photoactivation of the ground-state isomer and the photon
7 energy storage occur. The metastable-state isomer obtained in the photo-irradiated solution is
8 generally condensed by the solvent removal, then its isomerization energy is evaluated by a
9 calorimetric tool such as differential scanning calorimetry (DSC) which measures the
10 exothermicity of the reverse isomerization process from the metastable to ground-state form. The
11 solution-state compounds undergo a facile isomerization within the dilute condition in the absence
12 of steric hindrance which otherwise influences the photoswitching process particularly in
13 condensed phases.⁴⁷ The solution-state MOST materials, if highly concentrated, could be
14 integrated into a flow system for solar energy storage and heat release for various applications.^{8,48–}
15 50

16 Pristine norbornadiene/quadracyclane (NBD/QC) couple, which undergoes reversible σ
17 bond formation and dissociation, has a remarkable potential to store up to 0.97 MJ/kg, the highest

1 gravimetric energy density experimentally measured so far for MOST systems. The pristine NBD,
2 however, absorbs wavelengths below 250 nm in solution, which is a small fraction of solar
3 spectrum at sea level.³⁸ In order to utilize a wider range of solar spectrum, Moth-Poulsen and
4 coworkers developed NBD derivatives covalently functionalized with cyano and aromatic groups,
5 which forms a push-pull conjugated system and leads to a significantly red-shifted light absorption
6 compared to that of pristine NBD.³⁹ Among diverse electron-withdrawing groups, a cyano group
7 was selected due to its low molecular weight which doesn't compromise the gravimetric energy
8 storage density of the MOST system. On the side of the aromatic functional group, an ethynyl
9 linker was introduced to further extend the conjugated system and red-shift the absorption
10 wavelength to 398 nm. Despite the favorable optical property gained and the high isomerization
11 energy ($\Delta H_{\text{storage}}$ per molecule) obtained from the functionalization, the gravimetric energy
12 densities ($\Delta H_{\text{storage}}$ per weight) of the functionalized compounds were decreased due to the
13 increased molecular weight, particularly from the incorporation of aromatic functional groups.

14 In the pursuit of resolving this issue, a strategy of coupling one aromatic group to multiple
15 NBDs was developed.⁴⁰ This reduces the weight contribution of the shared donor (*i.e.* an aryl or
16 ethynyl-aryl group) to the molecular weight per NBD unit. The electronically-coupled
17 photoswitches exhibited similar thermal reversion barriers for QC-QC and QC-NBD isomeric
18 states. The isomerization energy per photoswitch of either dimer was similar to that of pristine
19 NBD/QC couple, while the larger molecular weight of the extended structure contributed to
20 lowering the gravimetric energy density of the dimeric form. Another molecular design which
21 contains two phenyl substituents on NBD unit also exhibited a similar level of red-shifted
22 absorption and $\Delta H_{\text{storage}}$ per molecule, while the substantial weight of two aryl groups significantly
23 reduced the gravimetric energy density of NBD.¹³

1 An interesting study experimented the impact of steric pressure within the photoswitch
2 structure imposed by a varied substituent R (H, Me, and *i*-Pr) on the light absorption of NBD and
3 thermal stability of QC.⁵¹ The increased steric bulk would push the C=C bonds closer to each other,
4 causing a slight red-shift of the absorption, reflected by both λ_{max} (240, 242, and 245 nm) and λ_{onset}
5 (391, 403, and 414 nm) of the derivatives in the order of increasing level of steric pressure. The
6 longer half-life of a more sterically hindered compound was attributed to the larger steric repulsion
7 in the NBD isomer than in the QC for such a compound, and the *i*-Pr NBD derivative was tested
8 in a flow device for effective photo-isomerization to its QC isomer (Figure 2a).

9 The isomerization of azobenzene derivatives and the associated energy change were first
10 studied by Yee and coworkers in 1983 using photometric calorimetry.⁵² Various structures with
11 electron donating and withdrawing substituents on the azobenzene scaffold were synthesized,
12 demonstrating the red-shift of the π - π^* absorption band from λ_{max} of 317 nm (pristine azobenzene)
13 up to 428 nm. The substituted structures exhibited a similar or greater energy storage density
14 compared to pristine azobenzene, except for the *ortho*-dimethyl substituted structure, which has a
15 low quantum yield of *E-Z* isomerization and results in a lower ΔH . Overall, the substituents
16 contributed to decreasing the thermal half-life of *cis* isomers by reducing the π electron density on
17 the azo group through electron delocalization.

18 The substitution of a phenyl group by a heteroaryl ring revealed to increase the PSS ratio
19 between *trans* and *cis* isomers under photo-irradiation.⁵³⁻⁵⁵ For pristine azobenzene, there is a
20 considerable overlap between the absorption of *trans* and *cis* isomers, leading to a suboptimal PSS
21 for either *trans*-to-*cis* or *cis*-to-*trans* conversion process (around 90%).⁵⁶ An arylazopyrazole
22 photochrome, on the other hand, displays widely separated λ_{max} of *trans* (328 nm) and *cis* (275
23 nm), and its *para*-methoxy derivative also shows the parted λ_{max} of *trans* (347 nm) and *cis* (281

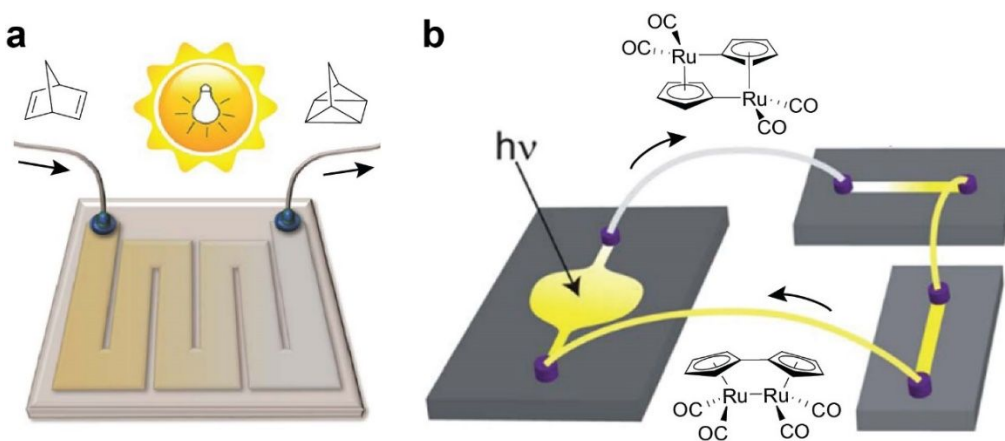
1 nm). This spectral separation between photoisomers leads to nearly quantitative photo-
2 isomerization in both directions (greater than 98%). In addition, the half-lives of *cis* isomers were
3 greatly prolonged to months and years, compared to those of azobenzene derivatives that span
4 from hours to days. The remarkable thermal stability of *cis* arylazopyrazole isomers was attributed
5 to the intramolecular C–H \cdots π interaction between the orthogonal pyrazole C–H group and phenyl
6 ring in the T-shaped *cis* conformation, which increases the reversion energy barrier. Furthermore,
7 the methoxy-substituted arylazopyrazole exhibits photoswitching in aqueous solutions due to the
8 increased polarity, which enables the potential application of thermal energy storage in a non-
9 volatile and environmentally-friendly medium.⁵⁷

10 The impact of London dispersion force on the isomerization energy was studied by Wegner
11 and coworkers, through the substitution of the bridging group between two azobenzene units.⁵⁸
12 Large cycloalkyl substituents were probed to increase the degree of London dispersion among
13 *trans* isomers, which contributed to raising the ΔH per azobenzene unit as well as the gravimetric
14 energy density of the MOST system.

15 Polymeric structures based on a poly(methacrylate) backbone and azobenzene side groups
16 were also developed to explore the correlation between steric effect and energy storage of MOST
17 systems.⁵⁹ The poly(methacrylate) displays a high syndiotacticity from radical polymerization,
18 bearing *syn* ester side groups spaced apart by 5 Å. The favorable steric effect that increases the
19 energy level of *cis* compared to *trans* state effectively enhanced the energy density of polymer (0.7
20 MJ/kg) by 3.8 times per azobenzene unit and 2.6 times per weight relative to the pristine
21 azobenzene. The incorporation of a large end group, such as hexa-*peri*-hexabenzocoronene (HBC),
22 was designed to facilitate a self-assembly of polymer into cylindrical structures to further enhance

1 the steric effect. However, the presence of photo-inactive end groups resulted in the significant
2 reduction of gravimetric energy density as well as the isomerization energy per azobenzene unit.

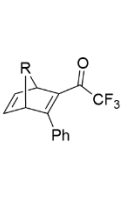
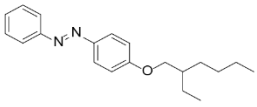
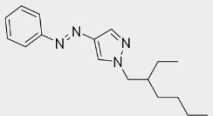
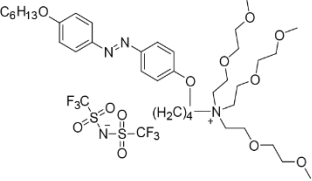
3 $\text{FvRu}_2(\text{CO})_4$ was particularly studied for the application in flow systems (Figure 2b).
4 Vollhardt and coworkers designed the alkyl-functionalized compounds to increase the solubility
5 of $\text{FvRu}_2(\text{CO})_4$: 22 g/L for pristine compound, 276 g/L with *t*-Bu substitution, and 400 g/L with
6 dodecyl chains demonstrated in THF.⁸ Despite the successful design strategy for solubility
7 enhancement, the large substituents compromised the gravimetric energy density of the system, as
8 also shown in NBD/QC and azobenzene counterparts.



9
10 **Figure 2.** A schematic illustration of flow systems developed for solution-state photon energy
11 storage with (a) NBD/QC and (b) $\text{FvRu}_2(\text{CO})_4$. Reproduced and adapted from Ref.[8,51] with
12 permission from The Royal Society of Chemistry.

13

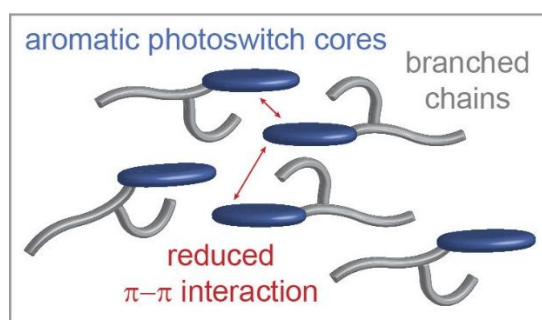
1 **3. Condensed liquid-state MOST compounds**2 **Table 2.** Liquid-state properties of MOST materials

Chemical Structure	MW (g/mol)	λ_{\max} (nm)	$\Delta H_{\text{storage}}$ (kJ/mol)	$\Delta H_{\text{storage}}$ (MJ/kg)	$t_{1/2}$ 298 K	Ref.
 1.  2.  3.  4. 	264	323	152	0.58	3.0 d	41
	290	342	103	0.35	5.3 d	
	292	323	49	0.17	3.5 d	
	318	326	48	0.15	2.0 d	
	310	344	52	0.17	16 h	62
	284	328	41	0.14	128 d	60
	957	356	52	0.05	/	61

3
4 /: unreported

5 The removal of solvent molecules that do not participate in the photo-isomerization process would
 6 greatly enhance the energy storage density of the MOST system. Therefore, building upon the
 7 fundamental characterizations of the optical and thermal properties of MOST compounds
 8 conducted in solution, the development of neat liquid phase MOST compounds has been pursued
 9 *via* structural designs that allow the compounds to exhibit melting points similar to or lower than
 10 room temperatures. Generally, the liquid phase of MOST compounds can be achieved by reducing
 11 the stacking of aromatic units in photochromic cores, particularly for planar molecules such as
 12 *trans* azoarenes. A prominent strategy is to install a branched alkyl or branched ethylene glycol
 13 chain to one of the aromatic rings to generate asymmetric structures where the flexible and bulky
 14 chains hinder the facile stacking between adjacent aromatic cores (Figure 3).^{60–62} Non-branched

1 linear alkyl chains with a limited degree of freedom are prone to generate crystalline MOST
2 compounds, which will be further illustrated in section 5, due to the planarity of alkyl-linked
3 aromatic molecules and the well-ordered stacking among the alkyl chains as well as between
4 aromatic cores.^{14,63–65} Therefore, it is essential to weaken both the π - π interaction and London
5 dispersion force among the neighboring molecules to produce a stable liquid phase with a low
6 melting point. For intrinsically non-planar photochromes, such as NBD, the presence of the
7 flexible branched chain is less crucial, yet desirable for generating liquid phase.

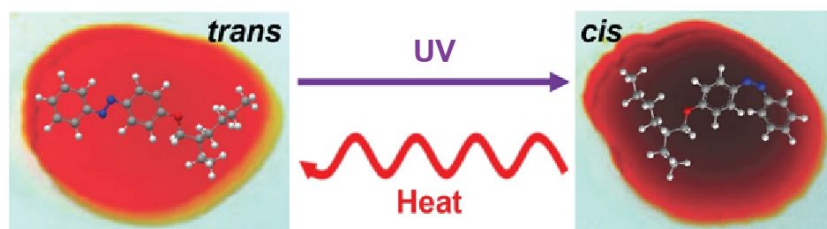


8

9 **Figure 3.** A schematic illustration of a liquid-phase MOST compound design

10 While pristine NBD is a liquid, most of the derivatives with red-shifted light absorption
11 are solids at room temperature, and their photoswitching properties have been primarily
12 characterized in dilute solutions. The photoswitching of a few NBD derivatives has been
13 performed in neat liquid phase, as illustrated in Table 2.⁴¹ The molecular designs build upon the
14 principles studied in solution state, incorporating a push-pull structure across a C=C bond and a
15 series of alkyl or cycloalkyl substituents on the NBD bridge, in order to red-shift the absorption
16 spectrum and to improve thermal stability of QC isomers. Surprisingly, the half-lives measured in
17 solution (2–5 days) were shortened to 2–205 min in neat liquid condition, due to the internal
18 thermal triggering of QC-to-NBD reversion and cascading isomerization in the condensed
19 environment.

1 To achieve a liquid phase of azobenzene and arylazopyrazole at room temperature, the
2 covalent attachment of a branched 2-ethylhexyl group was performed on phenyl and pyrazole
3 rings.^{60,62} Such a branched alkyl chain in a racemic form drastically weakened the intermolecular
4 interactions among the photochromic molecules, lowering their melting point for both *trans* and
5 *cis* isomers and allowing for their facile isomerization in the liquid phase (Figure 4). The 2-
6 ethylhexyl group was also selected for its low molecular weight compared to longer alkyl or
7 ethyleneglycol chains.⁶⁰ The incorporation of these heavier groups was demonstrated in the
8 structure of ammonium-based ionic compound, resulting in lowering its crystallinity due to the
9 flexibility and bulkiness of functional groups which weakened the π - π stacking and Madelung
10 energy of the structure. The counter anion Tf_2N^- , which exhibits the delocalized anionic charge,
11 was selected to lower the electrostatic interactions. The resulting ionic liquid showed similar level
12 of ΔH per azobenzene unit despite a much lower gravimetric energy density attributed to the
13 incorporated heavy substituents.⁶¹



14
15 **Figure 4.** Neat liquid state, reversible photo-isomerization of 2-ethylhexyl-substituted azobenzene.
16 Reproduced and adapted from Ref.[62] with permission from the The Royal Society of Chemistry.

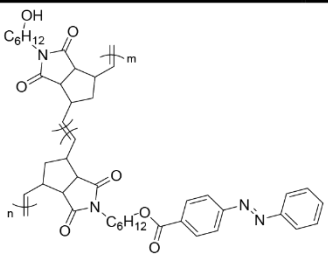
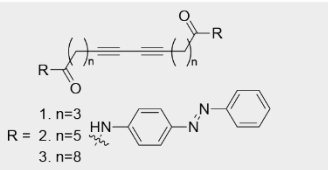
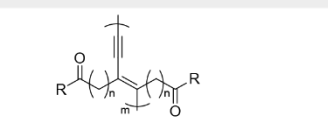
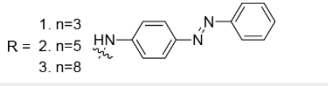
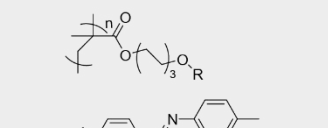
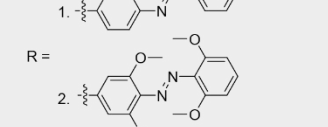
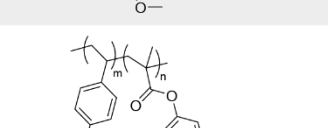
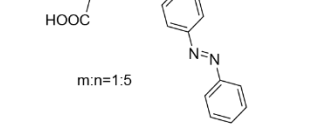
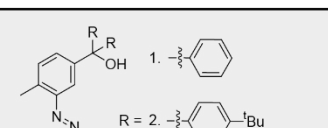
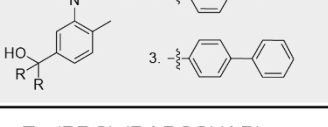
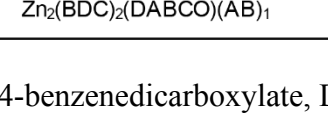
17

1 **4. Solid-state MOST compounds**2 **Table 3.** Solid-state properties of MOST materials

Chemical Structure	Per Unit MW (g/mol)	λ_{\max} (nm)	$\Delta H_{\text{storage}}$ (kJ/mol)	$\Delta H_{\text{storage}}$ (MJ/kg)	State (F/S/P)	$t_{1/2}$ 298 K	Ref.
	~573	380	224	0.39	F (20-30 μm)	52 d	66
			310	0.54	S (MeCN)		
	~618	374	216	0.35	F (15-35 μm)	/	67
			290	0.47	S (MeCN)	37 d	
	~507	410	193	0.38	F (100 μm)	12 d	68
	~533	391	266	0.50	S (MeCN)	52 d	69
	~251	360	94	0.37	S (DCM)	80 h	70
	~582	338	168	0.29	S (DMF)	55 d	71
	~598	354	132	0.22	F (~30 μm)	/	72
			173	0.29	S (EtOH)	16 h	
	~457	350	91	0.20	S (MeCN)	33 h	73

- 3
- 4 rGO: reduced graphene oxide, CNT: carbon nanotube, PPI: poly(propylene imine) dendrimer, F:
- 5 film, S: suspension, P: powder, /: unreported

1 **Table 3.** Solid-state properties of MOST materials (continued)

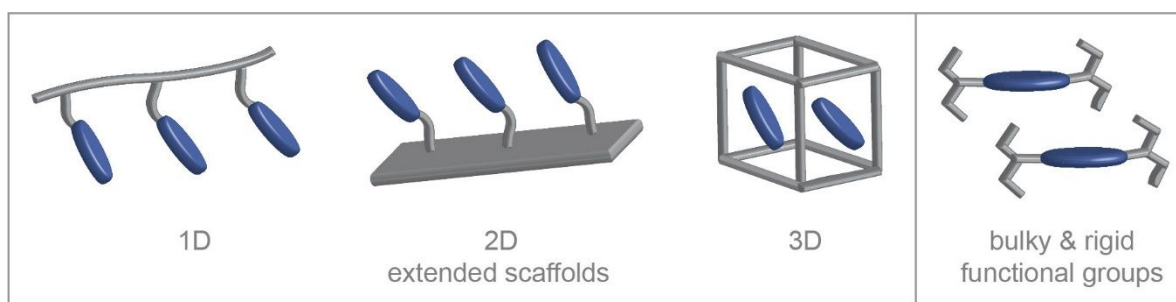
Chemical Structure	Per Unit MW (g/mol)	λ_{\max} (nm)	$\Delta H_{\text{storage}}$ (kJ/mol)	$\Delta H_{\text{storage}}$ (MJ/kg)	State (F/S/P)	$t_{1/2}$ 298 K	Ref.
	763	320	137	0.18	F (100 μm)	0.25 h	77
	290	360	61	0.21	/	/	
	318	360	73	0.23	S (DCM)	/	76
	360	360	80	0.22	/	28 h	
	290	~360	45	0.15	/	/	
	318	~360	51	0.16	S (DCM)	/	76
	360	~360	59	0.16	/	/	
	~380	351	48	0.12	F (35 nm)	12 h	74
	~486	323	8	0.02	F (20 nm)	16 h	
	~296	325	27	0.09	F (~250 nm)	75 h	75
	575	347	77	0.13	/	/	
	799	350	87	0.11	F (400–600 nm)	/	81
	879	350	88	0.10	/	/	
Zn ₂ (BDC) ₂ (DABCO)(AB) ₁	761	441	22	0.029	P	4.5 y	78

2

3 BDC: 1,4-benzenedicarboxylate, DABCO: 1,4-diazabicyclo[2.2.2]octane, AB: azobenzene, /: /

4 unreported

1 The design of solid-state MOST compounds has been achieved by incorporating photoswitches
2 onto several solid scaffolds, such as nanocarbon materials (*i.e.* reduced graphene oxide, rGO, or
3 carbon-nanotubes, CNTs),^{66–73} polymers,^{74–77} and metal organic frameworks (MOFs).⁷⁸ These
4 extended 1D, 2D, and 3D templates allow the MOST compounds to maintain a solid phase, either
5 as films, powders, or suspended solids, and enable the photoswitches to undergo isomerization
6 while attached on the extended scaffold (Figure 5). The templating strategy results in an array of
7 orderly packed photochromes that experience significant intermolecular interactions, which often
8 leads to the suppressed isomerization of photoswitches. Therefore, it is crucial to create a templated
9 structure that allows for a facile conformational change of photoswitches by providing
10 conformational freedom that is carefully designed and implemented. This has been accomplished
11 by fine-tuning the grafting density of azobenzene units on the scaffolds.



12
13 **Figure 5.** A schematic illustration of a solid-phase MOST material design

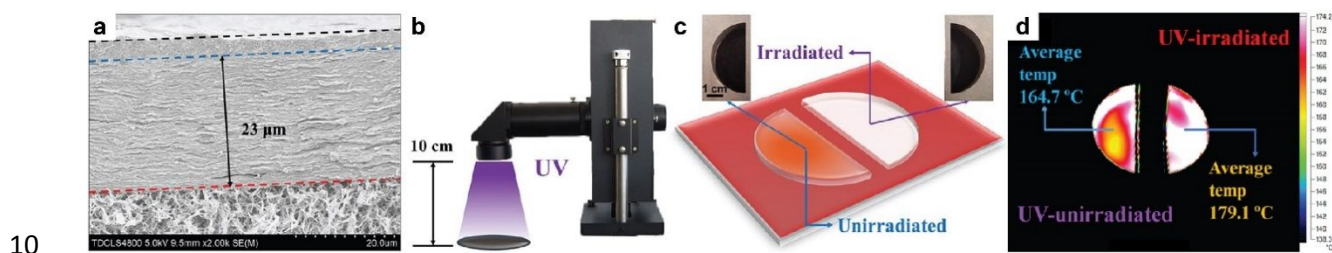
14 However, lowering the grafting density has implications, notably a lowered gravimetric
15 energy density of the MOST system. Polymeric backbones and carbon templates do not participate
16 in the photon energy storage, while significantly contributing to the overall mass of the material
17 systems. This leads to the development of strategies that optimize the loading density of
18 photoactive species on the polymer or carbon templates, which still enables the unhindered photo-
19 switching, induces favorable intermolecular interactions among the photoswitch side groups, and

1 mitigates the suboptimal gravimetric energy density lowered by the inclusion of large templates.
2 It is indeed a challenging quest to achieve a solid-state MOST system that exhibits a large
3 isomerization energy, a long half-life of *cis* isomer, and a high PSS ratio under illumination.
4 Nevertheless, many rGO or CNT-based MOST systems have been developed with an optimized
5 grafting density and reported to store up to 0.54 MJ/kg level of energy density.⁶⁶ Moreover, the
6 impact of the chromophore size and the presence of intermolecular H-bonds on the half-life of *cis*
7 isomers has been investigated.

8 In the absence of extended 1D, 2D, and 3D templates, it requires a different strategy to
9 fine-tune the spatial separation between the photoswitches in a condensed solid, since small
10 aromatic molecules are prone to crystallize, limiting the conformational freedom of switches. In
11 order to accomplish a MOST system based on small molecules operating in solid, the formation
12 of an amorphous phase is essential, enabled by the covalent functionalization of photoswitches
13 with bulky and rigid substituents (Figure 5). This strategy will be further discussed later in this
14 section.

15 Feng and coworkers demonstrated the templated photochrome assembly on rGO with
16 varied size of photochromic moieties.⁶⁶ The largest group contains three azobenzene units linked
17 to a central 1,3,5-benzenetricarboxamide, and such a bulky structure was grafted onto rGO at a
18 density of 1:68 (one group per 68 carbons) to achieve the highest energy density. It showed over
19 70% isomerization at PSS in a suspended solid state, a high energy density (0.54 MJ/kg), and a
20 long half-life of *cis* isomer (52 days). The facile isomerization in the suspended solid state is
21 attributed to the sufficient free volume around each photochrome, supported by the decreased PSS
22 ratio for a higher density sample at a 1:60 grafting ratio. The functionalized rGO MOST materials
23 were deposited on substrates as thin films and irradiated with UV, which led to a lower degree of

1 isomerization compared to the suspension state due to the increased steric hindrance in solid
2 materials without solvation. Another functional group with two azobenzene units linked to a 1,3-
3 benzene dicarboxamide moiety was functionalized onto rGO, which exhibited a reduced energy
4 density than the larger trimer counterpart.⁶⁷ The lower grafting density and the less steric
5 interaction among the photoswitches resulted in the suboptimal energy density as well as a shorter
6 half-life of *cis* isomers. The UV-irradiated films were monitored by IR thermography during the
7 thermally-activated reverse isomerization and the heat release. Compared to the identical film
8 without UV irradiation, the *cis*-rich sample exhibited ~14 °C higher temperature, demonstrating
9 the significant heat release from the isomerization (Figure 6).



11 **Figure 6.** (a) A cross-sectional SEM image of a film made of rGO-templated bisazobenzenes, (b)
12 a schematic illustration of UV irradiation setup, (c) irradiated and unirradiated samples, (d)
13 comparative IR thermographs of macroscopic heat release from the irradiated and unirradiated
14 samples upon the thermal triggering. Permission is granted subject to an appropriate
15 acknowledgement given to X. Zhao et al., *Controlling Heat Release from a Close -Packed*
16 *Bisazobenzene-Reduced - Graphene - Oxide Assembly Film for High - Energy Solid - State*
17 *Photothermal Fuels*, Wiley. Copyright 2017 Wiley-VCH Verlag GmbH & Co. KGaA, Weinheim.

18 In pursuit of lowering the *cis*-to-*trans* reverse isomerization energy barrier that requires
19 high temperature triggering conditions (over 100 °C for thermal reversion), prevalent in rGO-
20 templated MOST compounds, a push-pull azoheteroarene with an imidazole ring was

1 synthesized.⁶⁸ This design significantly reduces the half-life of *cis* isomer to 12 days, due to the
2 electron transfer from the methoxy groups to the imidazole ring, which decreases the bond order
3 of N=N and facilitates the molecular rotation. Similar rGO-templated azobenzene units with
4 methoxy and carboxylic acid functional groups, on the other hand, exhibited a much longer half-
5 life (52 days) caused by the intermolecular H-bonds among the neighboring COOH groups.^{68,69}

6 rGOs grafted with three-layer dendritic hyperbranched poly(propylene imine) containing
7 azobenzene units were also developed to increase the loading density of photoactive species in
8 MOST system.⁷⁰ The energy density of 0.37 MJ/kg was achieved due to the increased
9 intermolecular interactions among azobenzene units. Similarly, rGOs grafted with 1,3,5-triazine
10 branches functionalized two azobenzene units were developed to increase the loading density of
11 photoswitches. Due to the high grafting density and bundling effect, the *cis* isomers are greatly
12 stabilized, displaying a long half-life of 55 days.⁷¹

13 A push-pull structured azobenzene was also grafted on CNTs,⁷² exhibiting an appreciable
14 energy density and cyclability, with a shortened half-life of *cis* isomer compared to the pristine
15 azobenzene on CNT structures.⁷³ The steric strain generated by the CNT-templated structure
16 provides a high degree of intermolecular interactions between the azobenzene units, effectively
17 increasing the ΔH per azobenzene. However, due to the large template structure, the gravimetric
18 energy density remained in the range of 0.2–0.3 MJ/kg. In thin film experiments, the *cis*-rich and
19 *trans*-rich samples showed a temperature difference of 10 °C upon thermal triggering.

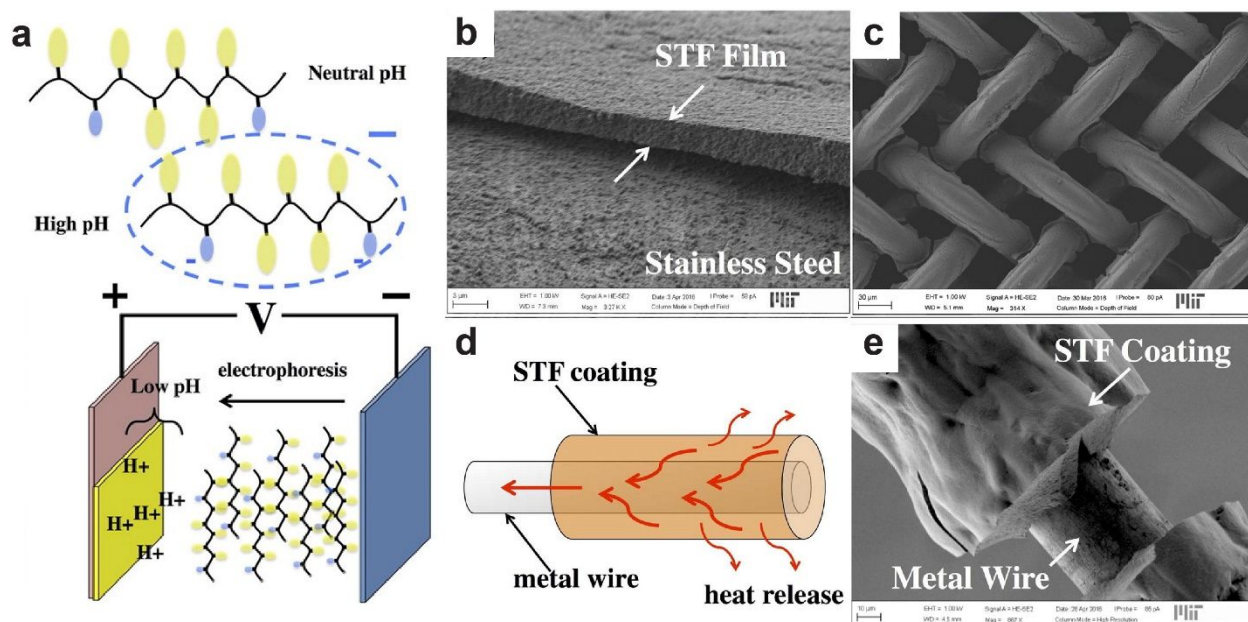
20 Polymer structures bearing photoswitch side groups are widely used to generate solid-state
21 MOST systems. Compared to the nanocarbon scaffold, polymer backbones are more flexible,
22 causing a lower degree of template-enforced steric interaction and more facile isomerization in
23 solid state. In addition, non-conjugated polymer backbones do not strongly absorb visible light, as

1 opposed to CNT and rGO, which generally increases the isomerization ratio at PSS. A
2 poly(norbornene) containing azobenzene side chains, for example, achieves a fair degree of *trans*-
3 *to-cis* isomerization (72%) at PSS.⁷⁷ The flexible polymeric MOST materials were stretched to
4 generate more free volume, leading to a higher PSS ratio (85%), a high ΔH per azobenzene unit
5 (137 kJ/mol), and more rapid *cis-to-trans* reverse isomerization under visible light irradiation (T_{\max}
6 reached in ~ 10 min) compared to the unstretched films. The thermal half-life of the polymer
7 measured in dark is 0.25 h at room temperature, which is much shorter than the half-lives of other
8 solid-state MOST materials.

9 Symmetric diacetylenes decorated with azobenzene side groups and their photo-
10 polymerized forms are crystalline solids that are insoluble in common organic solvents except for
11 DMF, due to the strong intermolecular interactions including H-bonds through amide linkages and
12 π - π interactions between azobenzene groups.⁷⁶ The solids suspended in organic solvents undergo
13 photo-switching and simultaneous dissolution into solvents, following the generation of polar *cis*
14 isomers with weakened intermolecular interactions. A much higher gravimetric energy density
15 was achieved with diacetylene-based MOST, compared to the poly(norbornene) counterpart,⁷⁷ due
16 to the compact template structure and the high loading of photochromes in the materials. The
17 polydiacetylenes obtained by the UV-induced topochemical polymerization of diacetylenes
18 exhibit reduced energy densities compared to the monomers, due to the restricted conformational
19 change of azobenzene units anchored on the rigid polymer backbones. It is notable that the role of
20 H-bonding moiety, the amide linkage, is essential in generating insoluble solids, corroborated by
21 a control experiment where the replacement of the amide group by an ester linkage drastically
22 increased the solubility of diacetylene and polydiacetylene MOST materials.

1 Poly(methyl methacrylate) structures decorated with azobenzene (PAzo) and *ortho*-
2 methoxy functionalized azobenzene side chains (PmAzo) were developed by Wu and coworkers
3 to achieve a stacked device structure which harvests a large fraction of solar spectrum.^{74,79,80}
4 Equipped with a blue-to-yellow down-converter filter as a top layer, which suppresses the
5 unwanted *cis*-to-*trans* reversion, the underlying layer of PmAzo effectively stores photon energy
6 in the visible light range. Another layer of UV pass filter allows the selective passage of UV
7 photons to the bottom layer of polymer with unfunctionalized azobenzene side chains for energy
8 storage. A considerable PSS ratio in solid state was achieved for PmAzo (73%) comparable to that
9 of solution-state photoswitching (72%), despite the decreased PSS ratio of PAzo in solid (24%)
10 compared to that of solution state (65%).

11 The challenge of depositing uniform films of MOST materials and controlling film
12 thickness was addressed by a design of ionic copolymer based on poly(methyl methacrylate)
13 backbone and side groups of azobenzene and benzoic acid (Figure 7a).⁷⁵ This allows for the
14 electrodeposition of a deprotonated polymer on conductive substrates, such as metal plates and
15 wire meshes (Figure 7b, 7c). The coated substrates enable the facile heat transfer from the MOST
16 films to metallic components (Figure 7d, 7e). In a thin-film condition, 43% of the PSS ratio was
17 achieved through direct irradiation on solid-state materials.



1
2 **Figure 7.** (a) A schematic illustration of the electrodeposition of a copolymer with azobenzene
3 and benzoic acid side groups. (b) A cross-sectional SEM image of an electrodeposited MOST (*i.e.*
4 STF) film on stainless steel substrate. (c) SEM image of 25 μm mesh coated with the MOST
5 polymer. (d) Concept of the stored heat released into a metal wire. (e) SEM image of an
6 electrodeposited film atop a 50 μm fiber. Reproduced and adapted with permission from Ref. [75].
7 Copyright 2016 American Chemical Society.

8
9 In the absence of nanocarbon or polymeric scaffolds, small molecules based on azobenzene
10 moiety tend to crystallize due to the strong aromatic stacking interactions. The functionalization
11 of pristine azobenzene with bulky substituents was demonstrated to effectively prevent the crystal
12 packing and form an amorphous solid state of photoswitching materials.¹² A *meta* position of each
13 phenyl group was functionalized with bulky aromatic substituents and an *ortho* position was
14 methyl-functionalized.⁸¹ The molecules were able to reversibly photoswitch in thin films upon the
15 exposure to photo-irradiations, exhibiting a high PSS *cis* ratio of 60% for compound 1, 80% for
16 compound 2, and 74% for compound 3, as a result of increased free volume around the
photochromes. In addition to the role of being spacer moieties, the bulky functional groups

1 increased the isomerization energy, ΔH per azobenzene unit, by imposing a large intramolecular
2 steric repulsion in *cis* form, which raises the energy level of *cis* isomer and increases the energy
3 difference between the *trans* and *cis* states. The ΔH per azobenzene unit increases with larger
4 substituents (phenyl < ^tBu phenyl < biphenyl), while the gravimetric energy density decreases due
5 to the high molecular weight of the larger molecules.

6 Metal-organic frameworks (MOFs) have been investigated as a porous medium that can
7 incorporate various photoswitches as guest molecules, side groups, or a part of framework
8 backbones, primarily to create photo-responsive sensing materials, optoelectronics, and erasable
9 inks.^{82–87} A recent report from Griffin and coworkers illustrated a solid-state MOST based on a
10 MOF scaffold with a chemical formula of $Zn_2(BDC)_2(DABCO)(AB)_x$ where x denotes an average
11 number of azobenzene loaded per unit cell.⁷⁸ Upon UV irradiation, 40% of the azobenzene guest
12 was switched to *cis* conformation, and 21 kJ/mol of thermal energy is calculated to be released by
13 the triggered *cis*-to-*trans* isomerization process ($x=1$). An extremely long half-life (4.5 years) of
14 azobenzene *cis* isomer was obtained in the confined environment, which is unique for a pristine
15 azobenzene structure.

16

1 **5. Phase transition MOST compounds**2 **Table 4. Thermal properties of phase transition MOST materials**

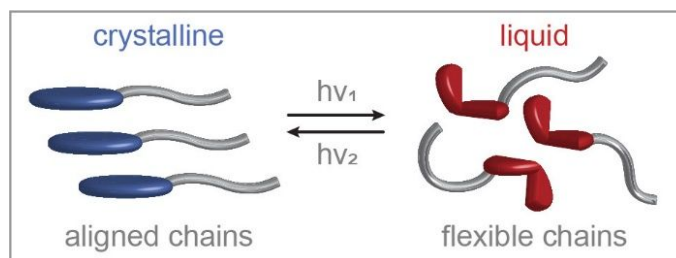
Chemical Structure	T_m (trans) (°C)	T_m (cis) (°C)	MW (g/mol)	ΔH_{iso} (MJ/kg)	ΔH_c (MJ/kg)	ΔH_{total} (MJ/kg)	ΔH_{total} (kJ/mol)	$t_{1/2}$ 298 K	Ref.
	93	27	286	0.18	0.15	0.33	94		
	82	25	284	0.19	0.14	0.33	94		
	1. m=6 2. n=6 3. n=7	83 83	35 312	0.18 0.17	0.16 0.16	0.34 0.33	101 103	~90 d	14
	4. n=8 5. n=10 6. n=11	88 92	340 354	0.16 0.16	0.18 0.20	0.34 0.36	116 127		
	1.	67	Liq	427	0.11	0.08	0.19	82	
	2.	91	53	398	0.11	0.12	0.23	92	
	3.	71	Liq	398	0.10	0.12	0.22	88	/
	4.	61	Liq	434	0.07	0.10	0.17	76	65
	1.	45	-36	466	0.05	0.10	0.15	70	2.0 y
	2.	56	-42	483	0.05	0.90	0.14	66	258 d
	3.	78	Liq	499	0.05	0.07	0.12	62	322 d
	1.	81	31	380	0.13	0.04	0.17	65	/
	2.	84	40	409	0.12	0.08	0.20	81	64
	1. -OC13H27 2. -OC15H31	65	/	713	0.18	0.03	0.21	151	32 h
	87	Liq	756	0.07	0.07	0.14	97	/	61

3

4 PPI: poly(propylene imine) dendrimer, /: unreported

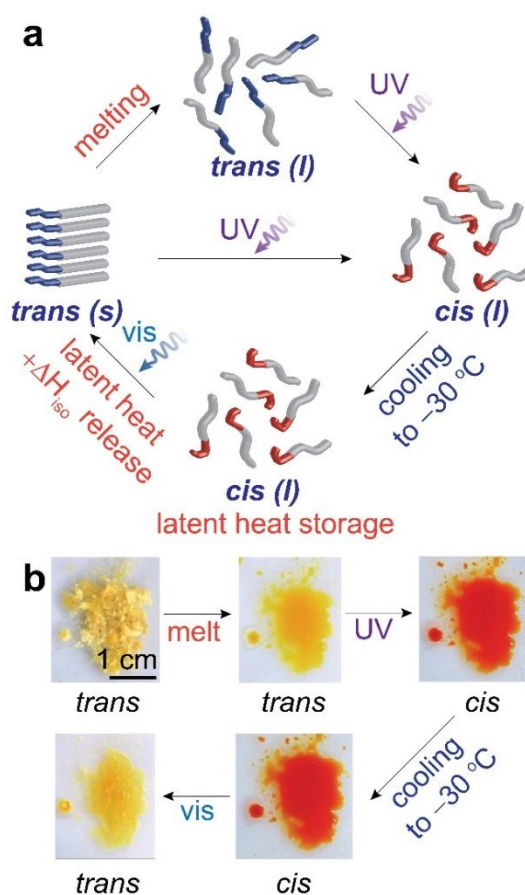
1 A recently developed strategy for increasing the energy storage in MOST systems involves a
2 design of photoswitches that undergo phase transitions during the structural isomerization. All of
3 the reported examples thus far incorporate azobenzene or azoheteroarene structures, which display
4 solid phase in the ground state (*trans*) and liquid phase in the metastable state (*cis*) due to the
5 increased polarity and sterics of the twisted *cis* isomeric form. In order to achieve a distinct phase
6 for each isomeric form, a significant structural change should occur during photo-isomerization
7 that induces crystalline packing in one isomer and disrupts the packing in the other isomeric form.
8 This requires the incorporation of a flexible, yet crystallizable, functional group to an aromatic
9 photoswitch system and has been primarily achieved with long alkyl functionality attached to an
10 azoarene core (Figure 8). Long alkyl chains crystallize at low temperatures due to the London
11 dispersion force, which scales with the length of chain, and melt at elevated temperatures to gain
12 flexibility and interact with non-planar aromatic cores.^{14,63–65} Other functional groups that display
13 such characteristics are anticipated to produce phase transition MOST compounds.^{61,88}

14 A schematic of the energy storage and release process is shown in Figure 9a, which
15 involves the absorption of thermal and photon energy by *trans* isomers in the process of generating
16 a stable liquid state of *cis* isomers. The unique feature of the phase change MOST materials is that
17 the crystallization energy is released concurrently with the release of isomerization energy during
18 the triggered *cis*-to-*trans* reverse transformation. Therefore, the total energy storage density
19 (ΔH_{total} in Table 4) is calculated as the sum of isomerization energy and the crystallization energy
20 of *trans* isomer. To maximize the total energy density, the molecular designs that increase the
21 crystallinity of *trans* isomer while maintaining the stable liquid phase of *cis* isomer in varied
22 temperature conditions were investigated.



1

2 **Figure 8.** A schematic illustration of a phase-transition MOST compound design



3

4 **Figure 9.** (a) A schematic illustration of latent heat and photon energy absorption by a phase
 5 change MOST, the energy storage in liquid phase, and the triggered release. (b) Series of optical
 6 images of a phase change MOST material that undergoes melting, UV irradiation, cooling, and
 7 visible-light-induced crystallization. Reproduced and adapted with permission from Ref. [65].

8 Copyright 2020 American Chemical Society.

1 Two phase-change MOST structures based on the arylazopyrazole with alkyl functional
2 groups were recently reported by multiple research groups of Li, Moth-Poulsen, Fuchter, and
3 Han.^{14,65} The alkyl group was functionalized on either the *para* position of phenyl ring or on a
4 nitrogen atom in the pyrazole group, and the length of the alkyl chain as well as other functional
5 groups on the photochrome were varied to modulate the phase transition enthalpy and the melting
6 point of *cis* isomers. The crystallization energy of *trans* isomers increases with the longer alkyl
7 chains (with or without an alkene end group) attached on the phenyl ring, which contributes to
8 enhancing the total energy storage density up to 0.36 MJ/kg. The series of compounds display
9 much lowered melting points of *cis* isomers compared to *trans* counterparts, and one compound
10 ($n = 8$) in particular showed a reversible photo-induced phase transition between solid (*trans*) and
11 liquid (*cis*) at room temperature due to the low melting point of the *cis* isomer (19 °C).¹⁴ The other
12 series of arylazopyrazole with the ester-linked alkyl chains on the pyrazole ring showed an
13 extremely stable liquid phase of *cis* isomers (*i.e.* no melting or crystallization in the range of -50
14 to 90 °C; marked as 'Liq' in Table 4), as a result of the functionalization. These three compounds
15 were demonstrated to store the liquid phase and the latent heat at temperatures much lower than 0
16 °C for a long-term storage up to a month, followed by the optically-triggered heat release at
17 temperatures as low as -30 °C (Figure 9b). This shows a potential of recycling waste heat and the
18 triggered release of the stored latent heat at an extremely cold climate.

19 A recent report demonstrated the design of a series of phase-change MOST compounds
20 that exhibit red-shifted $n-\pi^*$ absorption through the *ortho*-functionalization of azobenzene
21 moiety.⁶³ The fluorine, methoxy, and mixed halogen groups on the *ortho* positions of
22 photochromes, appended to a tridecanoate group, enabled the solid-to-liquid transition of materials
23 upon the exposure to low irradiance visible light, particularly sunlight through 530 nm, 590 nm,

1 and 625 nm bandpass filters. Despite the lower gravimetric energy densities, which arise from the
2 low ΔH_{iso} of *ortho*-functionalized azobenzenes, these new materials prove the concept of solar
3 heat and photon dual energy storage in phase change materials, accomplished under ambient or
4 greenhouse conditions in the absence of artificial UV light sources.

5 A similar design of azobenzene derivatives with ether-linked long alkyl chain was shown
6 to undergo photo-isomerization and concomitant phase transition at room temperature, displaying
7 a similar level of total energy density as the arylazopyrazole derivatives.⁶⁴ Poly(propylene imine)-
8 based dendrimers functionalized with azobenzene terminal groups also exhibited a photo-induced
9 solid-to-liquid phase transition which enabled the total energy storage of 0.21 MJ/kg.⁸⁸ An
10 ammonium-based ionic derivative of azobenzene with a bromide counter anion showed an ionic
11 crystalline phase as *trans* isomer and its transition to ionic liquid phase upon UV irradiation.⁶¹ This
12 shows the impact of the columbic interaction between the azobenzene-linked cation and the anion
13 on the phase of materials. The equivalent cationic compound with a larger anion with delocalized
14 charge (Tf_2N , see Table 2) was shown to form a liquid phase even as a *trans* isomer, thus its photo-
15 isomerization was performed in neat liquid phase. The ionic crystal-liquid phase crossover led to
16 storing a significant amount of thermal energy despite the large molecular weight of the structure.

17 All of the examples that we have illustrated here are single-component phase transition
18 MOST materials, while there is another class of MOST composite materials that incorporate
19 azobenzene derivatives as dopants in conventional phase change materials such as paraffins, fatty
20 acids, and fatty alcohols. The photo-responsive dopant molecules reversibly control the phase
21 transition of the composites, modulating the crystallization point of organic phase change materials
22 and extending the latent heat storage time of their liquid phase. The photo-regulation of the

1 supercooling of materials shows a unique way in which photoswitches are applied to control the
2 thermal energy storage in another material through intermolecular interactions.^{89–91}

3 **6. Conclusions and Future Directions**

4 The remarkable discoveries of MOST systems operating in diverse phases open up the
5 opportunities to apply a desired photoswitch system to an application that requires a specific phase
6 of materials. The design principles were established for *trans-cis* isomers and ring-opening-closing
7 photoswitches to result in the formation of liquid or solid phase, as well as the photo-induced phase
8 transitions. In general, the incorporation of large scaffolds such as nanocarbon or polymeric
9 backbone and bulky substituents leads to lower gravimetric energy densities despite the increased
10 isomerization energy per each photoswitch unit. Nevertheless, such functionalization tools are
11 essential for the generation of a particular phase that is desired for a flow system or film-based
12 thermal energy storage applications, which require the absence of volatile organic solvents or
13 photo-inactive components for maximizing the energy storage density. Other functional groups on
14 photochromes were investigated to alter the optical properties, notably by red-shifting the
15 absorption band from UV to visible light range, and to modulate the thermal half-life of metastable
16 isomers, which determines the energy storage time and the temperature at which the thermally-
17 activated reversion occurs.

18 The experimental MOST investigations thus far focused on NBD/QC, azobenzene, and
19 fulvalene dimetal complexes, and there are increasing attentions to developing novel
20 photoswitches that expand the scope of the current toolbox of MOST. For example, other
21 photoswitch systems including donor-acceptor Stenhouse adducts,^{92–99} hydrazones,^{100–104}
22 hemiindigos,^{105–107} and spiropyrans^{108–112} have shown outstanding success in applications such as
23 sensing, liquid crystal modulation, photo-responsive actuation, and cargo delivery, building upon

1 the thoroughly investigated optical properties in solutions and dispersions in a flexible medium.^{113–}
2 ¹¹⁷ The thermal characteristics of these switches are less explored than conventional MOST
3 compounds, partly due to the preliminary challenges including thermal decomposition or
4 insufficient isomerization energy of some candidates. Despite the challenges, the application of
5 strategies developed to overcome similar issues with pristine NBD or azobenzene, primarily the
6 covalent functionalization of photochromes with electron donating, withdrawing, or bulky
7 substituents, would potentially resolve the suboptimal thermal characteristics of other switches
8 with incredible potentials. Particularly, the intrinsic absorption of light in the visible range as well
9 as the negative photochromism of some photoswitches indicate a great potential as MOST
10 materials that harvest direct solar spectrum. Additionally, the experimental demonstration of
11 energy storage in DHA/VHF system is anticipated, based on their high isomerization energy
12 theoretically calculated.

13 Moreover, various design strategies applied to solution-state MOST materials will be
14 translated into neat liquid or solid phase systems, such as functionalization patterns that optimize
15 the light absorption, isomerization kinetics, or the degree of London dispersion forces, in order to
16 achieve devices with maximized solar spectrum harnessing, long-term energy storage, and
17 gravimetric energy density in the absence of solvents. Small azobenzene derivatives bearing
18 diverse electron donating or withdrawing groups, primarily studied in solutions for early research
19 in 1980s, are also expected to show interesting phase characteristics while maintaining a high level
20 of gravimetric energy densities due to their relatively low molecular weights. Lastly, the
21 integration of MOST systems into device structures will be considered when selecting a phase of
22 MOST materials for applications. In a device that utilizes inorganic catalysts or electrochemical
23 triggering methods, which assist the heat releasing process, the circulation of liquid phase or

1 solution-state MOST compounds over immobilized catalysts or electrode surface will be essential
2 for charging and discharging a large volume of materials. Photoactive thin-film coatings on
3 windows, windshields, or fabrics would require MOST materials that are insoluble in aqueous or
4 common organic solvents while displaying a significant light penetration depth through the coating
5 thickness. These specific requirements are currently explored to achieve practical MOST
6 applications that will be complementary tools to conventional solar energy conversion
7 technologies such as photovoltaics and solar fuel generations.

8

9 **Acknowledgements**

10 The research was supported by the SPROUT award (2019–042) from Brandeis Office of
11 Technology Licensing and Provost Research Award from Brandeis University. We also
12 acknowledge support from Brandeis NSF MRSEC, Bioinspired Soft Materials, DMR-2011486.
13 Y. S. thanks for the support from 2020 Division of Science Summer Undergraduate Research
14 Fellowship and Tema Nemtsov'79 and Professor Kraig Steffen Student Research Endowment
15 Fellowship

1 **References**

- 2 (1) Saritas, K.; Grossman, J. C. Accurate Isomerization Enthalpy and Investigation of the
3 Errors in Density Functional Theory for Dihydroazulene/Vinylheptafulvene
4 Photochromism Using Diffusion Monte Carlo. *J. Phys. Chem. C* **2017**, *121* (48), 26677–
5 26685. <https://doi.org/10.1021/acs.jpcc.7b09437>.
- 6 (2) Mogensen, J.; Christensen, O.; Kilde, M. D.; Abildgaard, M.; Metz, L.; Kadziola, A.;
7 Jevric, M.; Mikkelsen, K. V.; Nielsen, M. B. Molecular Solar Thermal Energy Storage
8 Systems with Long Discharge Times Based on the Dihydroazulene/Vinylheptafulvene
9 Couple. *European J. Org. Chem.* **2019**, *2019* (10), 1986–1993.
10 <https://doi.org/10.1002/ejoc.201801776>.
- 11 (3) Hansen, M. H.; Elm, J.; Olsen, S. T.; Gejl, A. N.; Storm, F. E.; Frandsen, B. N.; Skov, A.
12 B.; Nielsen, M. B.; Kjaergaard, H. G.; Mikkelsen, K. V. Theoretical Investigation of
13 Substituent Effects on the Dihydroazulene/Vinylheptafulvene Photoswitch: Increasing the
14 Energy Storage Capacity. *J. Phys. Chem. A* **2016**, *120* (49), 9782–9793.
15 <https://doi.org/10.1021/acs.jpca.6b09646>.
- 16 (4) Cacciarini, M.; Skov, A. B.; Jevric, M.; Hansen, A. S.; Elm, J.; Kjaergaard, H. G.;
17 Mikkelsen, K. V.; Brøndsted Nielsen, M. Towards Solar Energy Storage in the
18 Photochromic Dihydroazulene-Vinylheptafulvene System. *Chem. - A Eur. J.* **2015**, *21*
19 (20), 7454–7461. <https://doi.org/10.1002/chem.201500100>.
- 20 (5) Skov, A. B.; Broman, S. L.; Gertsen, A. S.; Elm, J.; Jevric, M.; Cacciarini, M.; Kadziola,
21 A.; Mikkelsen, K. V.; Nielsen, M. B. Aromaticity-Controlled Energy Storage Capacity of
22 the Dihydroazulene-Vinylheptafulvene Photochromic System. *Chem. - A Eur. J.* **2016**, *22*

- 1 (41), 14567–14575. <https://doi.org/10.1002/chem.201601190>.
- 2 (6) Kanai, Y.; Srinivasan, V.; Meier, S. K.; Vollhardt, K. P. C.; Grossman, J. C. Mechanism
3 of Thermal Reversal of the (Fulvalene)Tetracarbonyl-diruthenium Photoisomerization:
4 Toward Molecular Solar-Thermal Energy Storage. *Angew. Chemie - Int. Ed.* **2010**, *49*
5 (47), 8926–8929. <https://doi.org/10.1002/anie.201002994>.
- 6 (7) Börjesson, K.; Coso, D.; Gray, V.; Grossman, J. C.; Guan, J.; Harris, C. B.; Hertkorn, N.;
7 Hou, Z.; Kanai, Y.; Lee, D.; Lomont, J. P.; Majumdar, A.; Meier, S. K.; Moth-Poulsen,
8 K.; Myrabo, R. L.; Nguyen, S. C.; Segalman, R. A.; Srinivasan, V.; Tolman, W. B.;
9 Vinokurov, N.; Vollhardt, K. P. C.; Weidman, T. W. Exploring the Potential of Fulvalene
10 Dimetals as Platforms for Molecular Solar Thermal Energy Storage: Computations,
11 Syntheses, Structures, Kinetics, and Catalysis. *Chem. - A Eur. J.* **2014**, *20* (47), 15587–
12 15604. <https://doi.org/10.1002/chem.201404170>.
- 13 (8) Moth-Poulsen, K.; Coso, D.; Börjesson, K.; Vinokurov, N.; Meier, S. K.; Majumdar, A.;
14 Vollhardt, K. P. C.; Segalman, R. A. Molecular Solar Thermal (MOST) Energy Storage
15 and Release System. *Energy Environ. Sci.* **2012**, *5* (9), 8534–8537.
16 <https://doi.org/10.1039/c2ee22426g>.
- 17 (9) Bren, V. A.; Dubonosov, A. D.; Minkin, V. I.; Chernoiyanov, V. A. Norbornadiene–
18 Quadricyclane — an Effective Molecular System for the Storage of Solar Energy. *Russ.*
19 *Chem. Rev.* **1991**, *60* (5), 451–469. <https://doi.org/10.1070/rc1991v060n05abeh001088>.
- 20 (10) Dubonosov, A. D.; Bren, V. A.; Chernoiyanov, V. A. Norbornadiene–Quadricyclane as an
21 Abiotic System for the Storage of Solar Energy. *Russ. Chem. Rev.* **2002**, *71* (11), 917–
22 927. <https://doi.org/10.1070/rc2002v071n11abeh000745>.

- 1 (11) Lennartson, A.; Roffey, A.; Moth-Poulsen, K. Designing Photoswitches for Molecular
2 Solar Thermal Energy Storage. *Tetrahedron Lett.* **2015**, *56* (12), 1457–1465.
3 <https://doi.org/10.1016/j.tetlet.2015.01.187>.
- 4 (12) Dong, L.; Feng, Y.; Wang, L.; Feng, W. Azobenzene-Based Solar Thermal Fuels: Design,
5 Properties, and Applications. *Chem. Soc. Rev.* **2018**, *47* (19), 7339–7368.
6 <https://doi.org/10.1039/c8cs00470f>.
- 7 (13) Dreos, A.; Börjesson, K.; Wang, Z.; Roffey, A.; Norwood, Z.; Kushnir, D.; Moth-Poulsen,
8 K. Exploring the Potential of a Hybrid Device Combining Solar Water Heating and
9 Molecular Solar Thermal Energy Storage. *Energy Environ. Sci.* **2017**, *10* (3), 728–734.
10 <https://doi.org/10.1039/c6ee01952h>.
- 11 (14) Zhang, Z. Y.; He, Y.; Wang, Z.; Xu, J.; Xie, M.; Tao, P.; Ji, D.; Moth-Poulsen, K.; Li, T.
12 Photochemical Phase Transitions Enable Coharvesting of Photon Energy and Ambient
13 Heat for Energetic Molecular Solar Thermal Batteries That Upgrade Thermal Energy. *J.*
14 *Am. Chem. Soc.* **2020**, *142* (28), 12256–12264. <https://doi.org/10.1021/jacs.0c03748>.
- 15 (15) Petersen, A. U.; Hofmann, A. I.; Fillols, M.; Mansø, M.; Jevric, M.; Wang, Z.; Sumbly, C.
16 J.; Müller, C.; Moth-Poulsen, K. Solar Energy Storage by Molecular Norbornadiene–
17 Quadricyclane Photoswitches: Polymer Film Devices. *Adv. Sci.* **2019**, *6* (12).
18 <https://doi.org/10.1002/advs.201900367>.
- 19 (16) Hu, J.; Huang, S.; Yu, M.; Yu, H. Flexible Solar Thermal Fuel Devices: Composites of
20 Fabric and a Photoliquefiable Azobenzene Derivative. *Adv. Energy Mater.* **2019**, *9* (37),
21 1–10. <https://doi.org/10.1002/aenm.201901363>.
- 22 (17) Schalk, O.; Broman, S. L.; Petersen, M. Å.; Khakhulin, D. V.; Brogaard, R. Y.; Nielsen,

- 1 M. B.; Boguslavskiy, A. E.; Stolow, A.; Sølling, T. I. On the Condensed Phase Ring-
2 Closure of Vinylheptafulvalene and Ring-Opening of Gaseous Dihydroazulene. *J. Phys.*
3 *Chem. A* **2013**, *117* (16), 3340–3347. <https://doi.org/10.1021/jp400616c>.
- 4 (18) Görner, H.; Fischer, C.; Gierisch, S.; Daub, J. Dihydroazulene/Vinylheptafulvene
5 Photochromism: Effects of Substituents, Solvent, and Temperature in the
6 Photorearrangement of Dihydroazulenes to Vinylheptafulvenes. *J. Phys. Chem.* **1993**, *97*
7 (16), 4110–4117. <https://doi.org/10.1021/j100118a030>.
- 8 (19) Broman, S. L.; Jevric, M.; Nielsen, M. B. Linear Free-Energy Correlations for the
9 Vinylheptafulvene Ring Closure: A Probe for Hammett σ Values. *Chemistry - A European*
10 *Journal*. 2013, pp 9542–9548. <https://doi.org/10.1002/chem.201300167>.
- 11 (20) Mogensen, J.; Christensen, O.; Kilde, M. D.; Abildgaard, M.; Metz, L.; Kadziola, A.;
12 Jevric, M.; Mikkelsen, K. V.; Nielsen, M. B. Molecular Solar Thermal Energy Storage
13 Systems with Long Discharge Times Based on the Dihydroazulene/Vinylheptafulvene
14 Couple. *European J. Org. Chem.* **2019**, *2019* (10), 1986–1993.
15 <https://doi.org/10.1002/ejoc.201801776>.
- 16 (21) Lubrin, N. C. M.; Vlasceanu, A.; Frandsen, B. N.; Skov, A. B.; Kilde, M. D.; Mikkelsen,
17 K. V.; Nielsen, M. B. Dialkylated Dihydroazulene and Vinylheptafulvene Derivatives –
18 Synthesis and Switching Properties. *European J. Org. Chem.* **2017**, *2017* (20), 2932–
19 2939. <https://doi.org/10.1002/ejoc.201700446>.
- 20 (22) Olsen, S. T.; Elm, J.; Storm, F. E.; Gejl, A. N.; Hansen, A. S.; Hansen, M. H.; Nikolajsen,
21 J. R.; Nielsen, M. B.; Kjaergaard, H. G.; Mikkelsen, K. V. Computational Methodology
22 Study of the Optical and Thermochemical Properties of a Molecular Photoswitch. *J. Phys.*

- 1 *Chem. A* **2015**, *119* (5), 896–904. <https://doi.org/10.1021/jp510678u>.
- 2 (23) Kilde, M. D.; Mansø, M.; Ree, N.; Petersen, A. U.; Moth-Poulsen, K.; Mikkelsen, K. V.;
3 Nielsen, M. B. Norbornadiene-Dihydroazulene Conjugates. *Org. Biomol. Chem.* **2019**, *17*
4 (33), 7735–7746. <https://doi.org/10.1039/c9ob01545k>.
- 5 (24) Gertsen, A. S.; Olsen, S. T.; Broman, S. L.; Nielsen, M. B.; Mikkelsen, K. V. A DFT
6 Study of Multimode Switching in a Combined DHA/VHF-DTE/DHB System for Use in
7 Solar Heat Batteries. *J. Phys. Chem. C* **2017**, *121* (1), 195–201.
8 <https://doi.org/10.1021/acs.jpcc.6b10786>.
- 9 (25) Skov, A. B.; Petersen, J. F.; Elm, J.; Frandsen, B. N.; Santella, M.; Kilde, M. D.;
10 Kjaergaard, H. G.; Mikkelsen, K. V.; Nielsen, M. B. Towards Storage of Solar Energy in
11 Photochromic Molecules: Benzannulation of the Dihydroazulene/Vinylheptafulvene
12 Couple. *ChemPhotoChem* **2017**, *1* (5), 206–212. <https://doi.org/10.1002/cptc.201600046>.
- 13 (26) Kilde, M. D.; Arroyo, P. G.; Gertsen, A. S.; Mikkelsen, K. V.; Nielsen, M. B. Molecular
14 Solar Thermal Systems-Control of Light Harvesting and Energy Storage by
15 Protonation/Deprotonation. *RSC Adv.* **2018**, *8* (12), 6356–6364.
16 <https://doi.org/10.1039/c7ra13762a>.
- 17 (27) Vlasceanu, A.; Frandsen, B. N.; Skov, A. B.; Hansen, A. S.; Rasmussen, M. G.;
18 Kjaergaard, H. G.; Mikkelsen, K. V.; Nielsen, M. B. Photoswitchable Dihydroazulene
19 Macrocycles for Solar Energy Storage: The Effects of Ring Strain. *J. Org. Chem.* **2017**, *82*
20 (19), 10398–10407. <https://doi.org/10.1021/acs.joc.7b01760>.
- 21 (28) Brøndsted Nielsen, M.; Ree, N.; Mikkelsen, K. V.; Cacciarini, M. Tuning the
22 Dihydroazulene – Vinylheptafulvene Couple for Storage of Solar Energy. *Russ. Chem.*

- 1 *Rev.* **2020**, *89* (5), 573–586. <https://doi.org/10.1070/rcr4944>.
- 2 (29) Harpham, M. R.; Nguyen, S. C.; Hou, Z.; Grossman, J. C.; Harris, C. B.; Mara, M. W.;
3 Stickrath, A. B.; Kanai, Y.; Kolpak, A. M.; Lee, D.; Liu, D. J.; Lomont, J. P.; Moth-
4 Poulsen, K.; Vinokurov, N.; Chen, L. X.; Vollhardt, K. P. C. X-Ray Transient Absorption
5 and Picosecond IR Spectroscopy of Fulvalene(Tetracarbonyl)Diruthenium on
6 Photoexcitation. *Angew. Chemie - Int. Ed.* **2012**, *51* (31), 7692–7696.
7 <https://doi.org/10.1002/anie.201202952>.
- 8 (30) Vollhardt, K. P. C.; Weidman, T. W. Synthesis, Structure, and Photochemistry of
9 Tetracarbonyl(Fulvalene)Diruthenium. Thermally Reversible Photoisomerization
10 Involving Carbon-Carbon Bond Activation at a Dimetal Center. *J. Am. Chem. Soc.* **1983**,
11 *105* (6), 1676–1677. <https://doi.org/10.1021/ja00344a056>.
- 12 (31) Boese, R.; Cammack, J. K.; Matzger, A. J.; Pflug, K.; Tolman, W. B.; Vollhardt, K. P. C.;
13 Weidman, T. W. Photochemistry of (Fulvalene)Tetracarbonyldiruthenium and Its
14 Derivatives: Efficient Light Energy Storage Devices. *J. Am. Chem. Soc.* **1997**, *119* (29),
15 6757–6773. <https://doi.org/10.1021/ja9707062>.
- 16 (32) Cho, J.; Berbil-Bautista, L.; Pechenezhskiy, I. V.; Levy, N.; Meier, S. K.; Srinivasan, V.;
17 Kanai, Y.; Grossman, J. C.; Vollhardt, K. P. C.; Crommie, M. F. Single-Molecule-
18 Resolved Structural Changes Induced by Temperature and Light in Surface-Bound
19 Organometallic Molecules Designed for Energy Storage. *ACS Nano* **2011**, *5* (5), 3701–
20 3706. <https://doi.org/10.1021/nn2000367>.
- 21 (33) Hou, Z.; Nguyen, S. C.; Lomont, J. P.; Harris, C. B.; Vinokurov, N.; Vollhardt, K. P. C.
22 Switching from Ru to Fe: Picosecond IR Spectroscopic Investigation of the Potential of

- 1 the (Fulvalene)Tetracarbonyldiiron Frame for Molecular Solar-Thermal Storage. *Phys.*
2 *Chem. Chem. Phys.* **2013**, *15* (20), 7466–7469. <https://doi.org/10.1039/c3cp51292d>.
- 3 (34) Börjesson, K.; Lennartson, A.; Moth-Poulsen, K. Fluorinated Fulvalene Ruthenium
4 Compound for Molecular Solar Thermal Applications. *J. Fluor. Chem.* **2014**, *161*, 24–28.
5 <https://doi.org/10.1016/j.jfluchem.2014.01.012>.
- 6 (35) Hammond, G. S.; Wyatt, P.; DeBoer, C. D.; Turro, N. J. Photosensitized Isomerization
7 Involving Saturated Centers. *J. Am. Chem. Soc.* **1964**, *86* (12), 2532–2533.
8 <https://doi.org/10.1021/ja01066a056>.
- 9 (36) Harel, Y.; Adamson, A. W.; Kutal, C.; Grutsch, P. A.; Yasufuku, K. Photocalorimetry. 6.
10 Enthalpies of Isomerization of Norbornadiene and of Substituted Norbornadienes to
11 Corresponding Quadricyclenes. *J. Phys. Chem.* **1987**, *91* (4), 901–904.
12 <https://doi.org/10.1021/j100288a027>.
- 13 (37) Dauben, W. G.; Cargill, R. L. Photochemical Transformations-VIII. The Isomerization of
14 $\Delta^{2,5}$ -Bicyclo[2.2.1]Heptadiene to Quadricyclo[2.2.1.0^{2,6}.0^{3,5}]Heptane (Quadricyclene).
15 *Tetrahedron* **1961**, *15* (1–4), 197–201. [https://doi.org/10.1016/0040-4020\(61\)80026-4](https://doi.org/10.1016/0040-4020(61)80026-4).
- 16 (38) An, X. wu; Xie, Y. de. Enthalpy of Isomerization of Quadricyclane to Norbornadiene.
17 *Thermochim. Acta* **1993**, *220* (C), 17–25. [https://doi.org/10.1016/0040-6031\(93\)80451-F](https://doi.org/10.1016/0040-6031(93)80451-F).
- 18 (39) Quant, M.; Lennartson, A.; Dreos, A.; Kuisma, M.; Erhart, P.; Börjesson, K.; Moth-
19 Poulsen, K. Low Molecular Weight Norbornadiene Derivatives for Molecular Solar-
20 Thermal Energy Storage. *Chem. - A Eur. J.* **2016**, *22* (37), 13265–13274.
21 <https://doi.org/10.1002/chem.201602530>.

- 1 (40) Mansø, M.; Petersen, A. U.; Wang, Z.; Erhart, P.; Nielsen, M. B.; Moth-Poulsen, K.
2 Molecular Solar Thermal Energy Storage in Photoswitch Oligomers Increases Energy
3 Densities and Storage Times. *Nat. Commun.* **2018**, *9* (1), 1–7.
4 <https://doi.org/10.1038/s41467-018-04230-8>.
- 5 (41) Dreos, A.; Wang, Z.; Udmark, J.; Ström, A.; Erhart, P.; Börjesson, K.; Nielsen, M. B.;
6 Moth-Poulsen, K. Liquid Norbornadiene Photoswitches for Solar Energy Storage. *Adv.*
7 *Energy Mater.* **2018**, *8* (18), 1–9. <https://doi.org/10.1002/aenm.201703401>.
- 8 (42) Merino, E. Synthesis of Azobenzenes: The Coloured Pieces of Molecular Materials.
9 *Chem. Soc. Rev.* **2011**, *40* (7), 3835–3853. <https://doi.org/10.1039/c0cs00183j>.
- 10 (43) Bléger, D.; Hecht, S. Visible-Light-Activated Molecular Switches. *Angew. Chemie - Int.*
11 *Ed.* **2015**, *54* (39), 11338–11349. <https://doi.org/10.1002/anie.201500628>.
- 12 (44) Dong, M.; Babalhavaeji, A.; Samanta, S.; Beharry, A. A.; Woolley, G. A. Red-Shifting
13 Azobenzene Photoswitches for in Vivo Use. *Acc. Chem. Res.* **2015**, *48* (10), 2662–2670.
14 <https://doi.org/10.1021/acs.accounts.5b00270>.
- 15 (45) Yoshida, Z. ichi. New Molecular Energy Storage Systems. *J. Photochem.* **1985**, *29* (1–2),
16 27–40. [https://doi.org/10.1016/0047-2670\(85\)87059-3](https://doi.org/10.1016/0047-2670(85)87059-3).
- 17 (46) Börjesson, K.; Lennartson, A.; Moth-Poulsen, K. Efficiency Limit of Molecular Solar
18 Thermal Energy Collecting Devices. *ACS Sustain. Chem. Eng.* **2013**, *1* (6), 585–590.
19 <https://doi.org/10.1021/sc300107z>.
- 20 (47) Naito, T.; Horie, K.; Mita, I. Photochemistry in Polymer Solids. 11. The Effects of the
21 Size of Reaction Groups and the Mode of Photoisomerization on Photochromic Reactions

- 1 in Polycarbonate Film. *Macromolecules* **1991**, *24* (10), 2907–2911.
2 <https://doi.org/10.1021/ma00010a042>.
- 3 (48) Wang, Z.; Roffey, A.; Losantos, R.; Lennartson, A.; Jevric, M.; Petersen, A. U.; Quant,
4 M.; Dreos, A.; Wen, X.; Sampedro, D.; Börjesson, K.; Moth-Poulsen, K. Macroscopic
5 Heat Release in a Molecular Solar Thermal Energy Storage System. *Energy Environ. Sci.*
6 **2019**, *12* (1), 187–193. <https://doi.org/10.1039/c8ee01011k>.
- 7 (49) Wang, Z.; Udmark, J.; Börjesson, K.; Rodrigues, R.; Roffey, A.; Abrahamsson, M.;
8 Nielsen, M. B.; Moth-Poulsen, K. Evaluating Dihydroazulene/Vinylheptafulvene
9 Photoswitches for Solar Energy Storage Applications. *ChemSusChem* **2017**, *10* (15),
10 3049–3055. <https://doi.org/10.1002/cssc.201700679>.
- 11 (50) Wang, Z.; Losantos, R.; Sampedro, D.; Morikawa, M. A.; Börjesson, K.; Kimizuka, N.;
12 Moth-Poulsen, K. Demonstration of an Azobenzene Derivative Based Solar Thermal
13 Energy Storage System. *J. Mater. Chem. A* **2019**, *7* (25), 15042–15047.
14 <https://doi.org/10.1039/c9ta04905c>.
- 15 (51) Jorner, K.; Dreos, A.; Emanuelsson, R.; El Bakouri, O.; Galván, I. F.; Börjesson, K.;
16 Feixas, F.; Lindh, R.; Zietz, B.; Moth-Poulsen, K.; Ottosson, H. Unraveling Factors
17 Leading to Efficient Norbornadiene-Quadricyclane Molecular Solar-Thermal Energy
18 Storage Systems. *J. Mater. Chem. A* **2017**, *5* (24), 12369–12378.
19 <https://doi.org/10.1039/c7ta04259k>.
- 20 (52) Olmsted, J.; Lawrence, J.; Yee, G. G. Photochemical Storage Potential of Azobenzenes.
21 *Sol. Energy* **1983**, *30* (3), 271–274. [https://doi.org/10.1016/0038-092X\(83\)90156-1](https://doi.org/10.1016/0038-092X(83)90156-1).
- 22 (53) Otsuki, J.; Suwa, K.; Narutaki, K.; Sinha, C.; Yoshikawa, I.; Araki, K. Photochromism of

- 1 2-(Phenylazo)Imidazoles. *J. Phys. Chem. A* **2005**, *109* (35), 8064–8069.
2 <https://doi.org/10.1021/jp0531917>.
- 3 (54) Wendler, T.; Schütt, C.; Näther, C.; Herges, R. Photoswitchable Azoheterocycles via
4 Coupling of Lithiated Imidazoles with Benzenediazonium Salts. *J. Org. Chem.* **2012**, *77*
5 (7), 3284–3287. <https://doi.org/10.1021/jo202688x>.
- 6 (55) Weston, C. E.; Richardson, R. D.; Haycock, P. R.; White, A. J. P.; Fuchter, M. J.
7 Arylazopyrazoles: Azoheteroarene Photoswitches Offering Quantitative Isomerization and
8 Long Thermal Half-Lives. *J. Am. Chem. Soc.* **2014**, *136* (34), 11878–11881.
9 <https://doi.org/10.1021/ja505444d>.
- 10 (56) Fischer, E.; Frankel, M.; Wolovsky, R. Wavelength Dependence of Photoisomerization
11 Equilibria in Azocompounds. *J. Chem. Phys.* **1955**, *23* (7), 1367.
12 <https://doi.org/10.1063/1.1742302>.
- 13 (57) Nagai, Y.; Ishiba, K.; Yamamoto, R.; Yamada, T.; Morikawa, M.; Kimizuka, N.
14 Light-Triggered, Non-Centrosymmetric Self-Assembly of Aqueous Arylazopyrazoles at
15 the Air–Water Interface and Switching of Second-Harmonic Generation. *Angew. Chemie*
16 *Int. Ed.* **2021**, 1–7. <https://doi.org/10.1002/anie.202013650>.
- 17 (58) Kunz, A.; Heindl, A. H.; Dreos, A.; Wang, Z.; Moth-Poulsen, K.; Becker, J.; Wegner, H.
18 A. Intermolecular London Dispersion Interactions of Azobenzene Switches for Tuning
19 Molecular Solar Thermal Energy Storage Systems. *Chempluschem* **2019**, *84* (8), 1145–
20 1148. <https://doi.org/10.1002/cplu.201900330>.
- 21 (59) Jeong, S. P.; Renna, L. A.; Boyle, C. J.; Kwak, H. S.; Harder, E.; Damm, W.;
22 Venkataraman, D. High Energy Density in Azobenzene-Based Materials for Photo-

- 1 Thermal Batteries via Controlled Polymer Architecture and Polymer-Solvent Interactions.
2 *Sci. Rep.* **2017**, 7 (1). <https://doi.org/10.1038/s41598-017-17906-w>.
- 3 (60) Morikawa, M. A.; Yang, H.; Ishiba, K.; Masutani, K.; Hui, J. K. H.; Kimizuka, N. A
4 Liquid Arylazopyrazole Derivative as Molecular Solar Thermal Fuel with Long-Term
5 Thermal Stability. *Chem. Lett.* **2020**, 49 (6), 736–740. <https://doi.org/10.1246/cl.200171>.
- 6 (61) Ishiba, K.; Morikawa, M. A.; Chikara, C.; Yamada, T.; Iwase, K.; Kawakita, M.;
7 Kimizuka, N. Photoliquefiable Ionic Crystals: A Phase Crossover Approach for Photon
8 Energy Storage Materials with Functional Multiplicity. *Angew. Chemie - Int. Ed.* **2015**, 54
9 (5), 1532–1536. <https://doi.org/10.1002/anie.201410184>.
- 10 (62) Masutani, K.; Morikawa, M. A.; Kimizuka, N. A Liquid Azobenzene Derivative as a
11 Solvent-Free Solar Thermal Fuel. *Chem. Commun.* **2014**, 50 (99), 15803–15806.
12 <https://doi.org/10.1039/c4cc07713j>.
- 13 (63) Shi, Y.; Gerkman, M.; Qiu, Q.; Zhang, S.; Han, G. G. D. Sunlight-Activated Phase
14 Change Materials for Controlled Heat Storage and Triggered Release. *J. Mater. Chem. A*
15 **2021**. <https://doi.org/10.1039/D1TA01007G>.
- 16 (64) Liu, H.; Feng, Y.; Feng, W. Alkyl-Grafted Azobenzene Molecules for Photo-Induced Heat
17 Storage and Release via Integration Function of Phase Change and Photoisomerization.
18 *Compos. Commun.* **2020**, 21 (June), 100402. <https://doi.org/10.1016/j.coco.2020.100402>.
- 19 (65) Gerkman, M. A.; Gibson, R. S. L.; Calbo, J.; Shi, Y.; Fuchter, M. J.; Han, G. G. D.
20 Arylazopyrazoles for Long-Term Thermal Energy Storage and Optically Triggered Heat
21 Release below 0 °c. *J. Am. Chem. Soc.* **2020**, 142 (19), 8688–8695.
22 <https://doi.org/10.1021/jacs.0c00374>.

- 1 (66) Yang, W.; Feng, Y.; Si, Q.; Yan, Q.; Long, P.; Dong, L.; Fu, L.; Feng, W. Efficient
2 Cycling Utilization of Solar-Thermal Energy for Thermochromic Displays with
3 Controllable Heat Output. *J. Mater. Chem. A* **2019**, *7* (1), 97–106.
4 <https://doi.org/10.1039/c8ta05333b>.
- 5 (67) Zhao, X.; Feng, Y.; Qin, C.; Yang, W.; Si, Q.; Feng, W. Controlling Heat Release from a
6 Close-Packed Bisazobenzene–Reduced-Graphene-Oxide Assembly Film for High-Energy
7 Solid-State Photothermal Fuels. *ChemSusChem* **2017**, *10* (7), 1395–1404.
8 <https://doi.org/10.1002/cssc.201601551>.
- 9 (68) Yan, Q.; Zhang, Y.; Dang, Y.; Feng, Y.; Feng, W. Solid-State High-Power Photo Heat
10 Output of 4-((3,5-Dimethoxyaniline)-Diazenyl)-2- Imidazole/Graphene Film for
11 Thermally Controllable Dual Data Encoding/Reading. *Energy Storage Mater.* **2020**, *24*
12 (June 2019), 662–669. <https://doi.org/10.1016/j.ensm.2019.06.005>.
- 13 (69) Luo, W.; Feng, Y.; Qin, C.; Li, M.; Li, S.; Cao, C.; Long, P.; Liu, E.; Hu, W.; Yoshino,
14 K.; Feng, W. High-Energy, Stable and Recycled Molecular Solar Thermal Storage
15 Materials Using AZO/Graphene Hybrids by Optimizing Hydrogen Bonds. *Nanoscale*
16 **2015**, *7* (39), 16214–16221. <https://doi.org/10.1039/c5nr03558a>.
- 17 (70) Xu, X.; Wu, B.; Zhang, P.; Yu, H.; Wang, G. Molecular Solar Thermal Storage Enhanced
18 by Hyperbranched Structures. *Sol. RRL* **2020**, *4* (1).
19 <https://doi.org/10.1002/solr.201900422>.
- 20 (71) Feng, W.; Li, S.; Li, M.; Qin, C.; Feng, Y. An Energy-Dense and Thermal-Stable Bis-
21 Azobenzene/Hybrid Templated Assembly for Solar Thermal Fuel. *J. Mater. Chem. A*
22 **2016**, *4* (21), 8020–8028. <https://doi.org/10.1039/c6ta00221h>.

- 1 (72) Jiang, Y.; Huang, J.; Feng, W.; Zhao, X.; Wang, T.; Li, C.; Luo, W. Molecular Regulation
2 of Nano-Structured Solid-State AZO-SWCNTs Assembly Film for the High-Energy and
3 Short-Term Solar Thermal Storage. *Sol. Energy Mater. Sol. Cells* **2019**, *193* (January),
4 198–205. <https://doi.org/10.1016/j.solmat.2019.01.017>.
- 5 (73) Kucharski, T. J.; Ferralis, N.; Kolpak, A. M.; Zheng, J. O.; Nocera, D. G.; Grossman, J. C.
6 Templated Assembly of Photoswitches Significantly Increases the Energy-Storage
7 Capacity of Solar Thermal Fuels. *Nat. Chem.* **2014**, *6* (5), 441–447.
8 <https://doi.org/10.1038/nchem.1918>.
- 9 (74) Saydjari, A. K.; Weis, P.; Wu, S. Spanning the Solar Spectrum: Azopolymer Solar
10 Thermal Fuels for Simultaneous UV and Visible Light Storage. *Adv. Energy Mater.* **2017**,
11 *7* (3), 2–5. <https://doi.org/10.1002/aenm.201601622>.
- 12 (75) Zhitomirsky, D.; Grossman, J. C. Conformal Electroplating of Azobenzene-Based Solar
13 Thermal Fuels onto Large-Area and Fiber Geometries. *ACS Appl. Mater. Interfaces* **2016**,
14 *8* (39), 26319–26325. <https://doi.org/10.1021/acsami.6b08034>.
- 15 (76) Han, G. D.; Park, S. S.; Liu, Y.; Zhitomirsky, D.; Cho, E.; Dincă, M.; Grossman, J. C.
16 Photon Energy Storage Materials with High Energy Densities Based on Diacetylene-
17 Azobenzene Derivatives. *J. Mater. Chem. A* **2016**, *4* (41), 16157–16165.
18 <https://doi.org/10.1039/c6ta07086h>.
- 19 (77) Fu, L.; Yang, J.; Dong, L.; Yu, H.; Yan, Q.; Zhao, F.; Zhai, F.; Xu, Y.; Dang, Y.; Hu, W.;
20 Feng, Y.; Feng, W. Solar Thermal Storage and Room-Temperature Fast Release Using a
21 Uniform Flexible Azobenzene-Grafted Polynorborene Film Enhanced by Stretching.
22 *Macromolecules* **2019**, *52* (11), 4222–4231.

- 1 <https://doi.org/10.1021/acs.macromol.9b00384>.
- 2 (78) Griffiths, K.; Halcovitch, N. R.; Griffin, J. M. Long-Term Solar Energy Storage under
3 Ambient Conditions in a MOF-Based Solid-Solid Phase-Change Material. *Chem. Mater.*
4 **2020**, *32* (23), 9925–9936. <https://doi.org/10.1021/acs.chemmater.0c02708>.
- 5 (79) Zhou, H.; Xue, C.; Weis, P.; Suzuki, Y.; Huang, S.; Koynov, K.; Auernhammer, G. K.;
6 Berger, R.; Butt, H. J.; Wu, S. Photoswitching of Glass Transition Temperatures of
7 Azobenzene-Containing Polymers Induces Reversible Solid-to-Liquid Transitions. *Nat.*
8 *Chem.* **2017**, *9* (2), 145–151. <https://doi.org/10.1038/NCHEM.2625>.
- 9 (80) Weis, P.; Wang, D.; Wu, S. Visible-Light-Responsive Azopolymers with Inhibited π - π
10 Stacking Enable Fully Reversible Photopatterning. *Macromolecules* **2016**, *49* (17), 6368–
11 6373. <https://doi.org/10.1021/acs.macromol.6b01367>.
- 12 (81) Cho, E. N.; Zhitomirsky, D.; Han, G. G. D.; Liu, Y.; Grossman, J. C. Molecularly
13 Engineered Azobenzene Derivatives for High Energy Density Solid-State Solar Thermal
14 Fuels. *ACS Appl. Mater. Interfaces* **2017**, *9* (10), 8679–8687.
15 <https://doi.org/10.1021/acsami.6b15018>.
- 16 (82) Rice, A. M.; Martin, C. R.; Galitskiy, V. A.; Berseneva, A. A.; Leith, G. A.; Shustova, N.
17 B. Photophysics Modulation in Photoswitchable Metal-Organic Frameworks. *Chem. Rev.*
18 **2020**, *120* (16), 8790–8813. <https://doi.org/10.1021/acs.chemrev.9b00350>.
- 19 (83) Kanj, A. B.; Müller, K.; Heinke, L. Stimuli-Responsive Metal-Organic Frameworks with
20 Photoswitchable Azobenzene Side Groups. *Macromol. Rapid Commun.* **2018**, *39* (1), 1–
21 14. <https://doi.org/10.1002/marc.201700239>.

- 1 (84) Dolgoplova, E. A.; Rice, A. M.; Martin, C. R.; Shustova, N. B. Photochemistry and
2 Photophysics of MOFs: Steps towards MOF-Based Sensing Enhancements. *Chem. Soc.*
3 *Rev.* **2018**, *47* (13), 4710–4728. <https://doi.org/10.1039/c7cs00861a>.
- 4 (85) Williams, D. E.; Martin, C. R.; Dolgoplova, E. A.; Swifton, A.; Godfrey, D. C.;
5 Ejegbavwo, O. A.; Pellechia, P. J.; Smith, M. D.; Shustova, N. B. Flipping the Switch:
6 Fast Photoisomerization in a Confined Environment. *J. Am. Chem. Soc.* **2018**, *140* (24),
7 7611–7622. <https://doi.org/10.1021/jacs.8b02994>.
- 8 (86) Heinke, L. Diffusion and Photoswitching in Nanoporous Thin Films of Metal-Organic
9 Frameworks. *J. Phys. D. Appl. Phys.* **2017**, *50* (19). [https://doi.org/10.1088/1361-](https://doi.org/10.1088/1361-6463/aa65f8)
10 [6463/aa65f8](https://doi.org/10.1088/1361-6463/aa65f8).
- 11 (87) Williams, D. E.; Rietman, J. A.; Maier, J. M.; Tan, R.; Greytak, A. B.; Smith, M. D.;
12 Krause, J. A.; Shustova, N. B. Energy Transfer on Demand: Photoswitch-Directed
13 Behavior of Metal-Porphyrin Frameworks. *J. Am. Chem. Soc.* **2014**, *136* (34), 11886–
14 11889. <https://doi.org/10.1021/ja505589d>.
- 15 (88) Xu, X.; Zhang, P.; Wu, B.; Xing, Y.; Shi, K.; Fang, W.; Yu, H.; Wang, G. Photochromic
16 Dendrimers for Photoswitched Solid-To-Liquid Transitions and Solar Thermal Fuels. *ACS*
17 *Appl. Mater. Interfaces* **2020**, *12* (44), 50135–50142.
18 <https://doi.org/10.1021/acsami.0c14160>.
- 19 (89) Han, G. G. D.; Deru, J. H.; Cho, E. N.; Grossman, J. C. Optically-Regulated Thermal
20 Energy Storage in Diverse Organic Phase-Change Materials. *Chem. Commun.* **2018**, *54*
21 (76), 10722–10725. <https://doi.org/10.1039/C8CC05919E>.
- 22 (90) Han, G. G. D.; Li, H.; Grossman, J. C. Optically-Controlled Long-Term Storage and

- 1 Release of Thermal Energy in Phase-Change Materials. *Nat. Commun.* **2017**, *8* (1).
2 <https://doi.org/10.1038/s41467-017-01608-y>.
- 3 (91) Liu, H.; Tang, J.; Dong, L.; Wang, H.; Xu, T.; Gao, W.; Zhai, F.; Feng, Y.; Feng, W.
4 Optically Triggered Synchronous Heat Release of Phase-Change Enthalpy and Photo-
5 Thermal Energy in Phase-Change Materials at Low Temperatures. *Adv. Funct. Mater.*
6 **2021**, *31* (6), 1–11. <https://doi.org/10.1002/adfm.202008496>.
- 7 (92) Helmy, S.; Oh, S.; Leibfarth, F. A.; Hawker, C. J.; Read De Alaniz, J. Design and
8 Synthesis of Donor-Acceptor Stenhouse Adducts: A Visible Light Photoswitch Derived
9 from Furfural. *J. Org. Chem.* **2014**, *79* (23), 11316–11329.
10 <https://doi.org/10.1021/jo502206g>.
- 11 (93) Hemmer, J. R.; Poelma, S. O.; Treat, N.; Page, Z. A.; Dolinski, N. D.; Diaz, Y. J.;
12 Tomlinson, W.; Clark, K. D.; Hooper, J. P.; Hawker, C.; Read De Alaniz, J. Tunable
13 Visible and Near Infrared Photoswitches. *J. Am. Chem. Soc.* **2016**, *138* (42), 13960–
14 13966. <https://doi.org/10.1021/jacs.6b07434>.
- 15 (94) Ulrich, S.; Hemmer, J. R.; Page, Z. A.; Dolinski, N. D.; Rifaie-Graham, O.; Bruns, N.;
16 Hawker, C. J.; Boesel, L. F.; Read De Alaniz, J. Visible Light-Responsive DASA-
17 Polymer Conjugates. *ACS Macro Lett.* **2017**, *6* (7), 738–742.
18 <https://doi.org/10.1021/acsmacrolett.7b00350>.
- 19 (95) Hemmer, J. R.; Page, Z. A.; Clark, K. D.; Stricker, F.; Dolinski, N. D.; Hawker, C. J.;
20 Read De Alaniz, J. Controlling Dark Equilibria and Enhancing Donor-Acceptor Stenhouse
21 Adduct Photoswitching Properties through Carbon Acid Design. *J. Am. Chem. Soc.* **2018**,
22 *140* (33), 10425–10429. <https://doi.org/10.1021/jacs.8b06067>.

- 1 (96) Seshadri, S.; Gockowski, L. F.; Lee, J.; Sroda, M.; Helgeson, M. E.; Read de Alaniz, J.;
2 Valentine, M. T. Self-Regulating Photochemical Rayleigh-Bénard Convection Using a
3 Highly-Absorbing Organic Photoswitch. *Nat. Commun.* **2020**, *11* (1).
4 <https://doi.org/10.1038/s41467-020-16277-7>.
- 5 (97) Sroda, M. M.; Stricker, F.; Peterson, J. A.; Bernal, A.; Read de Alaniz, J. Donor–Acceptor
6 Stenhouse Adducts: Exploring the Effects of Ionic Character. *Chem. - A Eur. J.* **2020**.
7 <https://doi.org/10.1002/chem.202005110>.
- 8 (98) Mostafavi, S. H.; Li, W.; Clark, K. D.; Stricker, F.; Alaniz, J. R. De; Bardeen, C. J.
9 Photoinduced Deadhesion of a Polymer Film Using a Photochromic Donor-Acceptor
10 Stenhouse Adduct. *Macromolecules* **2019**, *52* (16), 6311–6317.
11 <https://doi.org/10.1021/acs.macromol.9b00882>.
- 12 (99) Lui, B. F.; Tierce, N. T.; Tong, F.; Sroda, M. M.; Lu, H.; Read De Alaniz, J.; Bardeen, C.
13 J. Unusual Concentration Dependence of the Photoisomerization Reaction in Donor-
14 Acceptor Stenhouse Adducts. *Photochem. Photobiol. Sci.* **2019**, *18* (6), 1587–1595.
15 <https://doi.org/10.1039/c9pp00130a>.
- 16 (100) Ryabchun, A.; Li, Q.; Lancia, F.; Aprahamian, I.; Katsonis, N. Shape-Persistent Actuators
17 from Hydrazone Photoswitches. *J. Am. Chem. Soc.* **2019**, *141* (3), 1196–1200.
18 <https://doi.org/10.1021/jacs.8b11558>.
- 19 (101) Iagatti, A.; Shao, B.; Credi, A.; Ventura, B.; Aprahamian, I.; Di Donato, M. Ultrafast
20 Processes Triggered by One- And Two-Photon Excitation of a Photochromic and
21 Luminescent Hydrazone. *Beilstein J. Org. Chem.* **2019**, *15*, 2438–2446.
22 <https://doi.org/10.3762/bjoc.15.236>.

- 1 (102) Zheng, L. Q.; Yang, S.; Lan, J.; Gyr, L.; Goubert, G.; Qian, H.; Aprahamian, I.; Zenobi,
2 R. Solution Phase and Surface Photoisomerization of a Hydrazone Switch with a Long
3 Thermal Half-Life. *J. Am. Chem. Soc.* **2019**, *141* (44), 17637–17645.
4 <https://doi.org/10.1021/jacs.9b07057>.
- 5 (103) Shao, B.; Qian, H.; Li, Q.; Aprahamian, I. Structure Property Analysis of the Solution and
6 Solid-State Properties of Bistable Photochromic Hydrazones. *J. Am. Chem. Soc.* **2020**, *141*
7 (20), 8364–8371. <https://doi.org/10.1021/jacs.9b03932>.
- 8 (104) Shao, B.; Aprahamian, I. Planarization-Induced Activation Wavelength Red-Shift and
9 Thermal Half-Life Acceleration in Hydrazone Photoswitches. *ChemistryOpen* **2020**, *9* (2),
10 191–194. <https://doi.org/10.1002/open.201900340>.
- 11 (105) Carrascosa, E.; Petermayer, C.; Scholz, M. S.; Bull, J. N.; Dube, H.; Bieske, E. J.
12 Reversible Photoswitching of Isolated Ionic Hemiindigos with Visible Light.
13 *ChemPhysChem* **2020**, *21* (7), 680–685. <https://doi.org/10.1002/cphc.201900963>.
- 14 (106) Petermayer, C.; Dube, H. Circular Dichroism Photoswitching with a Twist: Axially Chiral
15 Hemiindigo. *J. Am. Chem. Soc.* **2018**, *140* (42), 13558–13561.
16 <https://doi.org/10.1021/jacs.8b07839>.
- 17 (107) Petermayer, C.; Thumser, S.; Kink, F.; Mayer, P.; Dube, H. Hemiindigo: Highly Bistable
18 Photoswitching at the Biooptical Window. *J. Am. Chem. Soc.* **2017**, *139* (42), 15060–
19 15067. <https://doi.org/10.1021/jacs.7b07531>.
- 20 (108) Mostafavi, S. H.; Tong, F.; Dugger, T. W.; Kisailus, D.; Bardeen, C. J. Noncovalent
21 Photochromic Polymer Adhesion. *Macromolecules* **2018**, *51* (6), 2388–2394.
22 <https://doi.org/10.1021/acs.macromol.8b00036>.

- 1 (109) Özçoban, C.; Halbritter, T.; Steinwand, S.; Herzig, L. M.; Kohl-Landgraf, J.; Askari, N.;
2 Groher, F.; Fürtig, B.; Richter, C.; Schwalbe, H.; Suess, B.; Wachtveitl, J.; Heckel, A.
3 Water-Soluble Py-BIPS Spiroyrans as Photoswitches for Biological Applications. *Org.*
4 *Lett.* **2015**, *17* (6), 1517–1520. <https://doi.org/10.1021/acs.orglett.5b00397>.
- 5 (110) Nourmohammadian, F.; Abdi, A. A. Development of Molecular Photoswitch with Very
6 Fast Photoresponse Based on Asymmetrical Bis-Azospiropyran. *Spectrochim. Acta - Part*
7 *A Mol. Biomol. Spectrosc.* **2016**, *153*, 53–62. <https://doi.org/10.1016/j.saa.2015.07.110>.
- 8 (111) Ma, T.; Walko, M.; Lepoitevin, M.; Janot, J. M.; Balanzat, E.; Kocer, A.; Balme, S.
9 Combining Light-Gated and PH-Responsive Nanopore Based on PEG-Spiroyrans
10 Functionalization. *Adv. Mater. Interfaces* **2018**, *5* (2).
11 <https://doi.org/10.1002/admi.201701051>.
- 12 (112) Qu, L.; Xu, X.; Song, J.; Wu, D.; Wang, L.; Zhou, W.; Zhou, X.; Xiang, H. Solid-State
13 Photochromic Molecular Switches Based on Axially Chiral and Helical Spiroyrans. *Dye.*
14 *Pigment.* **2020**, *181*. <https://doi.org/10.1016/j.dyepig.2020.108597>.
- 15 (113) Petermayer, C.; Dube, H. Indigoid Photoswitches: Visible Light Responsive Molecular
16 Tools. *Acc. Chem. Res.* **2018**, *51* (5), 1153–1163.
17 <https://doi.org/10.1021/acs.accounts.7b00638>.
- 18 (114) Minkin, V. I. Light-Controlled Molecular Switches Based on Bistable Spirocyclic Organic
19 and Coordination Compounds. *Russ. Chem. Rev.* **2013**, *82* (1), 1–26.
20 <https://doi.org/10.1070/rc2013v082n01abeh004336>.
- 21 (115) Cardano, F.; Frascioni, M.; Giordani, S. Photo-Responsive Graphene and Carbon
22 Nanotubes to Control and Tackle Biological Systems. *Front. Chem.* **2018**, *6* (APR).

- 1 <https://doi.org/10.3389/fchem.2018.00102>.
- 2 (116) Lerch, M. M.; Szymański, W.; Feringa, B. L. The (Photo)Chemistry of Stenhouse
3 Photoswitches: Guiding Principles and System Design. *Chem. Soc. Rev.* **2018**, *47* (6),
4 1910–1937. <https://doi.org/10.1039/c7cs00772h>.
- 5 (117) Shao, B.; Aprahamian, I. Hydrazones as New Molecular Tools. *Chem* **2020**, *6* (9), 2162–
6 2173. <https://doi.org/10.1016/j.chempr.2020.08.007>.
- 7